Mixed-integer Linear Programming Models and Algorithms for Generation and Transmission Expansion Planning of Power Systems

Can Li[a], Antonio J. Conejo[b,c], Peng Liu[d], Benjamin P. Omell[d], John D. Siirola[e], Ignacio E. Grossmann[a,*]

[a]*Department of Chemical Engineering, Carnegie Mellon University, 5000 Forbes Ave, Pittsburgh, PA 15213, USA*
[b]*Department of Integrated Systems Engineering, The Ohio State University, 1971 Neil Avenue, Columbus, OH 43210, USA*
[c]*Department of Electrical and Computer Engineering, The Ohio State University, 2015 Neil Avenue, Columbus, OH 43210, USA*
[d]*National Energy Technology Laboratory, Pittsburgh, PA 15236, United States*
[e]*Center for Computing Research, Sandia National Laboratories, P.O. 5800, Albuquerque, NM, 87185, USA*

Abstract

With the increasing penetration of renewable generating units, especially in remote areas not well connected with load demand, there are growing interests to co-optimize generation and transmission expansion planning (GTEP) in power systems. Due to the volatility in renewable generation, a planner needs to include the operating decisions into the planning model to guarantee feasibility. However, solving the GTEP problem with hourly operating decisions throughout the planning horizon is computationally intractable. Therefore, we propose several spatial and temporal simplifications to the problem. Built on the generation expansion planning (GEP) formulation of Lara et al. (2018), we propose a mixed-integer linear programming formulation for the GTEP problem. Three different formulations, i.e., a big-M formulation, a hull formulation, and an alternative big-M formulation, are reported for transmission expansion. We theoretically compare the tightness of the LP relaxations of the three formu-

*Corresponding author
Email addresses: canl1@andrew.cmu.edu (Can Li), conejo.1@osu.edu (Antonio J. Conejo), Peng.Liu@netl.doe.gov (Peng Liu), Benjamin.Omell@netl.doe.gov (Benjamin P. Omell), jdsiiro@sandia.gov (John D. Siirola), grossmann@cmu.edu (Ignacio E. Grossmann)

lations. The proposed MILP GTEP model typically involves millions or tens of millions of variables, which makes the model not directly solvable by the commercial solvers. To address this computational challenge, we propose a nested decomposition algorithm and a tailored Benders decomposition algorithm that exploit the structure of the GTEP problem. Using a case study from ERCOT (Electric Reliability Council of Texas), we are able to show that the proposed tailored Benders decomposition outperforms the nested Benders decomposition. The coordination in the optimal generation and transmission expansion decisions from the ERCOT study implies that there is an additional value in solving GEP and TEP simultaneously.

Keywords: Power Systems, Renewable, Generation Transmission Expansion, Mixed-integer Programming, Decomposition Algorithm

1. Introduction

Generation expansion planning (GEP) of power systems involves determining the optimal size, location, and construction time of new power generation plants, while minimizing the total cost over a long-term planning horizon [1, 2]. There is a growing interest to use mathematical programming models to solve generation expansion planning problems [3, 4, 5]. Conventional power units are dispatchable thermal power plants that can provide stable power output. Due to computational tractability concerns, generation expansion models could ignore short-term operating decisions. However, with the increased penetration of renewable generation technologies, such as solar and wind, power systems nowadays need to be more flexible so as to adjust to the volatile power generation from renewables. In this case, operations decisions, such as unit commitment, ramping decisions, become important to assess system feasibility [6, 7, 8, 9, 10, 11, 12, 3, 13]. Due to the incorporation of short-term operating constraints into the long-term planning problem, the integrated model is computationally challenging. In order to solve such multi-scale problem efficiently, Lara et al. [3] use nested Benders decomposition to solve a GEP model with

unit commitment. Lohmann and Rebennack [13] develop a tailored Generalized Benders Decomposition algorithm.

Transmission expansion planning (TEP) refers to installing new transmission lines or expanding the capacities of existing transmission lines in a power system. Bahiense et al. [14] propose a mixed integer disjunctive model for transmission network expansion. [15] propose an MILP model that considers losses and guarantees convergence to optimality for the TEP. Zhang et al. [16] propose an improved model that includes a linear representation of reactive power, off-nominal bus voltage magnitudes and network losses. For a more detailed review of of TEP models and algorithms, we refer the readers to the review paper [17].

GEP and TEP are generally solved as two independent optimization problems since the market agents addressing these two problems are different. GEP pertains to producers, while TEP pertains to a regulated planner. However, the significant penetration of renewables into power systems may lead to their concentration in remote areas not well connected to load demand [2]. Therefore, installing renewables in those remote areas could compromise transmission expansion. The recognition of transmission's interaction with generation expansion has motivated the development of co-optimization methods to consider the tradeoffs between generation and transmission expansion [18]. Several works have been reported to simultaneously optimize generation and transmission expansion planning (GTEP) [19, 20]. We refer to Table 1 of the review paper [2] for a long list of works.

A number of related works consider uncertainties in the planning problem using two-stage or multistage stochastic programming [21, 22, 23], robust optimization [24, 25]. [26, 19] apply game theory or multi-level optimization to characterize the interaction of the participants in the markets.

This paper is an extension of the GEP model reported in [3] to a GTEP model. In [3], the authors propose an MILP model for deterministic generation expansion planning problem that represents the hourly operating decisions of the generators and storage units. Renewable generation and load data on some representative days are used as the input to the hourly unit commitment model

[27]. Lara et al. [3] use a tailored nested Benders decomposition algorithm to solve the multi-scale GEP problem. However, in [3] transmission expansion planning is not considered and the power flow equations ignore Kirchhoff's voltage law. In this paper, we extend the model in [3] by considering transmission expansion and DC power flow equations. We investigate three different formulations for transmission expansion, i.e., big-M formulation, hull formulation, and an alternative big-M formulation proposed by Bahiense et al. [14]. The proposed GTEP model is computationally more challenging to solve than the GEP model in [3]. To characterize the proposed solution approaches, we compare the nested Benders algorithm and a tailored Benders decomposition algorithm for the new GTEP model. The case study demonstrates the importance of the coordination between the generation and the transmission decisions in the optimal solution.

The rest of this paper is organized as follows. In section 2, we give the description and the assumptions of the problem that we address. In section 3, we describe the MILP formulation for our GTEP model. In section 4, we describe two solution techniques, a nested Benders decomposition and a tailored Benders decomposition. In section 5, a case study from ERCOT is used to illustrate the working of the model and the efficiency of the solution techniques. We draw the conclusion in section 6

2. Problem Statement and Assumptions

Given is a geographical region with existing and potential generating units and transmissions lines. The problem consists in making capacity expansion decisions for both generation and transmission while considering the unit commitment and power flow constraints at the operational level.

2.1. Generation representation

The existing and potential generation technologies are similar to the ones used in [3], i.e.,

- For the existing generators we consider: (a) coal: steam turbine (coal-st-old); (b) natural gas: boiler plants with steam turbine (ng-st-old), combustion turbine (ng-ct-old), and combined-cycle (ng-cc-old); (c) nuclear: steam turbine (nuc-st-old); (d) solar: photo-voltaic (pv-old); (e) wind: wind turbine (wind-old).

- For the potential generators we consider: (a) coal: without (coal-new) and with carbon capture (coal-ccs-new); (b) natural gas: combustion turbine (ng-ct-new), combined-cycle without (ng-cc-new) and with carbon capture (ng-cc-ccs-new); (c) nuclear: steam turbine (nuc-st-new); (d) solar: photo-voltaic (pv- new) and concentrated solar power (csp-new); (e) wind: wind turbine (wind-new).

Also known are: the generating units' nameplate (maximum) capacity; expected lifetime; fixed and variable operating costs; fixed and variable start-up cost; cost for extending their lifetimes; CO_2 emission factor and carbon tax, if applicable; fuel price, if applicable; and operating characteristics such as ramp-up/ramp-down rates, operating limits, contribution to spinning and quick start fraction for thermal generators, and capacity factor for renewable generators.

For the case of existing generators, their age at the beginning of the study horizon and location are also known. For the case of potential generators, the capital cost and the maximum yearly installation of each generation technology are also given. Also given is a set of potential storage units, with specified technology (e.g., lithium ion, lead-acid, and flow batteries), capital cost, power rating, rated energy capacity, charge and discharge efficiency, and storage lifetime. Additionally, the projected load demand is given for each location.

We assume that the generators using the same type of technology are homogeneous, i.e., their design parameters are identical. For example, all the coal-st-old generators have the same parameters, which can be obtained by performing aggregation on the existing generators that use coal steam turbines. Note that although the renewable generators of the same technology have the same design parameters under our assumption, they can have different capacity

factors depending on the weather conditions of the region in which they are installed.

2.2. Transmission representation

Given are existing and candidate transmission lines between any of the two neighboring buses. The susceptance, distance, and capacity of each transmission line are known. For the existing transmission lines, we assume that they will not reach their life expectancy during the planning horizon, i.e., we do not consider the retirement of transmission lines. For the candidate transmission lines, the capital cost of each transmission line is known.

We use DC power flow equations to calculate the power flow in each transmission line. These equations are built based on Kirchhoffs voltage and current laws which differ from the network flow model used in the work of Lara et al. [3].

2.3. Temporal representation

The GTEP model integrates unit commitment decisions to evaluate the hourly operation requirements. Given that the planning horizon of the GTEP problem can be as long as 10 to 30 years, solving the long-term planning problem with operating decisions in every hour of the planning horizon is intractable. Therefore, a simplification is needed to make the problem solvable, while representing the hourly fluctuations of the load and renewable profiles.

Several works propose to select a few representative days [27, 28, 29] from the full data set to represent the hourly fluctuations. The time series corresponding to the representative days are usually selected using some clustering algorithms, such as k-means, and hierarchical clustering. After performing the clustering on the full time series data set, the time series corresponding to the representative days are the centroids or medoids the clusters. In this paper, we use the package TimeSeriesClustering.jl developed by Teichgraeber and Brandt [28] to identify representative days in our data set.

2.4. Spatial representation

GTEP is typically performed on large scale power systems which consists of thousands of buses, such as ERCOT, SPP, PJM, MISO, etc. In most cases, it is intractable for GTEP to model each bus. Therefore, we adopt a similar approach as in [3] to reduce the spatial complexity of the problem. The area of interest is divided into several regions that have similar climate (e.g., wind speed and solar incidence over time), and load profiles. As we describe in the generation representation subsection, all the generators using the same technology have the same parameters. On the other hand, for the renewable generators, the capacity factors are dependent on the location at which they are installed. We assume that the capacity factors of the renewable generators in the same region are the same.

We assume that all the generators and loads are located at the center of each region. Since each region is treated as one bus in the power flow model, we only consider the tielines between two neighboring regions. We assume that the two ends of each tieline are the centers of the two regions it connects. All the tielines are assumed to have the same voltage, susceptance, and capacity. An example of the proposed spatial representation approach is shown in Figure 1. The ERCOT region is divided into five regions, Panhandle, Northeast, West, South, and Coast. The center of each region is specified as one of the cities in the region. The existing transmission lines are represented as solid lines while the candidate transmission lines are represented as dashed lines. Each region has generator clusters corresponding to different technologies.

2.5. Decisions and objective

With the above input data, spatial and temporal representations, the proposed GTEP model is to decide: a) when and where to install new generators, storage units and transmission lines; b) when to retire generators and storage units; c) whether or not to extend the life of the generators that reached their expected lifetime; d) unit commitment of the thermal generators during the representative days; e) power generations of the generator clusters and power

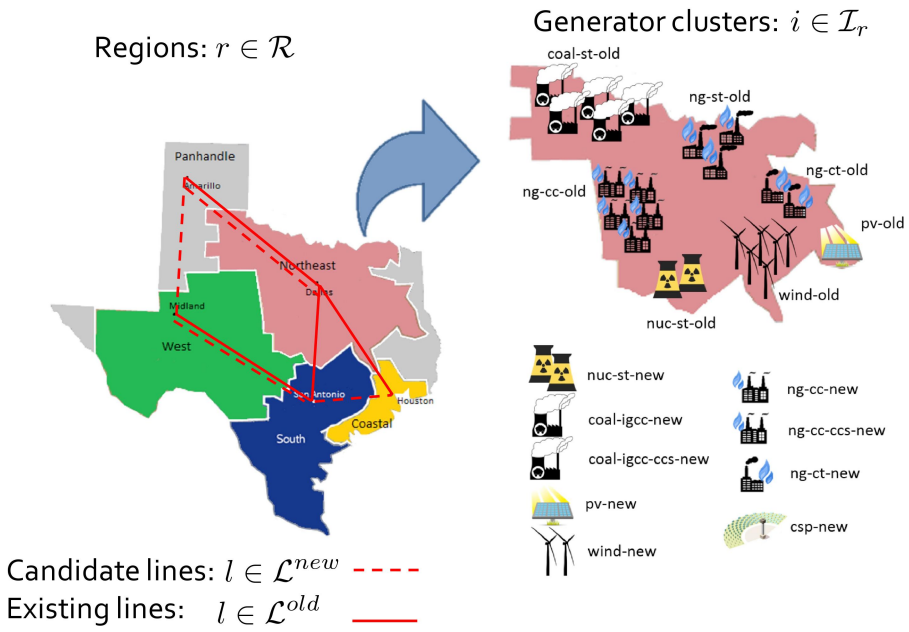

Figure 1: Spatial representation of the five ERCOT regions' generator clusters and transmission lines

flows through the transmission lines. The objective is to minimize the overall cost including operating, investment, and environmental costs.

3. MILP Formulation

This section presents a deterministic MILP formulation for the GTEP problem. Most of the MILP formulation is similar to that in [3]. Here, we emphasize the transmission expansion formulation that is added. Note that if an index appears in a summation or next to a $\forall$ symbol without a set, all elements in the corresponding set should be considered. The nomenclature for sets, parameters, and variables used in the MILP formulation are provided in Appendix B.

3.1. Transmission expansion constraints

Transmission line balance constraints. Variable $ntb_{l,t}$ denotes whether or not candidate transmission line l is built in year t. Variable $nte_{l,t}$ denotes

whether transmission line l has been installed in year t. Equation (1) represents the balance of transmission lines.

$$nte_{l,t} = nte_{l,t-1} + ntb_{l,t} \quad \forall l \in \mathcal{L}^{\text{new}}, t \tag{1}$$

The DC transmission constraints calculate and limit the power flows through the transmission lines. Parameter B_l represents the susceptance of line l. $\theta_{s(l),t,d,s}$, $\theta_{r(l),t,d,s}$ are the phase angles of the buses that are the sending-end and the receiving-end of line l, respectively, in year t, representative day d, and sub-period (hour) s. The existing transmission lines have to satisfy the DC power flow equation (2).

$$p^{\text{flow}}_{l,t,d,s} = B_l\big(\theta_{s(l),t,d,s} - \theta_{r(l),t,d,s}\big) \quad \forall l \in \mathcal{L}^{\text{old}}, t, d, s \tag{2}$$

The power flow through each transmission line is bounded. Parameter $F^{\max}_l$ represents the capacity of transmission line l. Thus:

$$-F^{\max}_l \le p^{\text{flow}}_{l,t,d,s} \le F^{\max}_l \quad \forall l \in \mathcal{L}^{\text{old}}, t, d, s \tag{3}$$

For the candidate transmission lines, we can write the following disjunction, where $NTE_{l,t}$ is a logic variable whose value can be True or False indicating whether or not transmission line l is installed in year t. If line l already exists in year t, the corresponding power flow has to satisfy DC power flow equation and upper and lower bounds. Otherwise, the corresponding power flow is zero.

$$\begin{bmatrix} NTE_{l,t} \\ p^{\text{flow}}_{l,t,d,s} = B_l(\theta_{s(l),t,d,s} - \theta_{r(l),t,d,s}) \\ -F^{\max}_l \le p^{\text{flow}}_{l,t,d,s} \le F^{\max}_l \end{bmatrix} \vee \begin{bmatrix} \neg NTE_{l,t} \\ p^{\text{flow}}_{l,t,d,s} = 0 \end{bmatrix} \quad \forall l \in \mathcal{L}^{\text{new}}, t, d, s \tag{4}$$

Standard approaches, i.e., big-M reformulation and convex hull reformulation [30], are available to reformulate disjunctions (4) into mixed integer constraints.

The big-M formulation of the disjunction is,

$$-M_l(1-nte_{l,t}) \leq p^{\text{flow}}_{l,t,d,s} - B_l(\theta_{s(l),t,d,s} - \theta_{r(l),t,d,s}) \leq M_l(1-nte_{l,t}) \quad \forall l \in \mathcal{L}^{\text{new}}, t, d, s \tag{5}$$

$$-F^{\max}_l nte_{l,t} \leq p^{\text{flow}}_{l,t,d,s} \leq F^{\max}_l nte_{l,t} \quad \forall l \in \mathcal{L}^{\text{new}}, t, d, s \tag{6}$$

This big-M formulation most commonly used in the literature [1] for TEP.

The hull formulation is,

$$p^{\text{flow}}_{l,t,d,s} = B_l \Delta\theta^1_{l,t,d,s} \quad \forall l \in \mathcal{L}^{\text{new}}, t, d, s \tag{7}$$

$$\theta_{s(l),t,d,s} - \theta_{r(l),t,d,s} = \Delta\theta^1_{l,t,d,s} + \Delta\theta^2_{l,t,d,s} \quad \forall l \in \mathcal{L}^{\text{new}}, t, d, s \tag{8}$$

$$-\pi \cdot nte_{l,t} \leq \Delta\theta^1_{l,t,d,s} \leq \pi \cdot nte_{l,t} \quad \forall l \in \mathcal{L}^{\text{new}}, t, d, s \tag{9}$$

$$-\pi(1 - nte_{l,t}) \leq \Delta\theta^2_{l,t,d,s} \leq \pi(1 - nte_{l,t}) \quad \forall l \in \mathcal{L}^{\text{new}}, t, d, s \tag{10}$$

where $\Delta\theta^1_{l,t,d,s}$ and $\Delta\theta^2_{l,t,d,s}$ are disaggregated variables for the angle difference of transmission line l. Variable $\Delta\theta^1_{l,t,d,s}$ is equal to the angle difference if transmission line l has been installed in year t. Otherwise, $\Delta\theta^2_{l,t,d,s}$ equals to the angle difference. In addition to equations (7)-(10), equation (6) needs to be included in the hull formulation.

The hull formulation has more continuous variables than the big-M formulation but it avoids using the big-M parameters of equations (5). Therefore, the hull formulation can provide tighter LP relaxation at the expense of solving larger LPs at each node of a branch-and-bound algorithm.

Alternative big-M formulation: Besides the big-M and hull formulations, an alternative big-M formulation is proposed by Bahiense et al. [14]. In this formulation, additional continuous variables $p^{\text{flow}+}_{l,t,d,s}$, $p^{\text{flow}-}_{l,t,d,s}$, $\Delta\theta^+_{l,t,d,s}$, $\Delta\theta^-_{l,t,d,s}$, are

introduced, where the superscript '+' means that the flow is in the same direction as the nominal direction of transmission line l, i.e., from the sending-end node $s(l)$ to the receiving-end node $r(l)$; superscript '-' means the opposite direction. By defining these new continuous variables, equation (5) is replaced by equations (11) to (14) and equation (6) is replaced by equations (17) and (18). Bahiense et al. [14] claim that the alternative big-M formulation is tighter than the big-M formulation. However, we prove that they have the same feasible region if we project the feasible region of the alternative big-M formulation onto the space of $(p^{\text{flow}}_{l,t,d,s}, \theta_{s(l),t,d,s}, \theta_{r(l),t,d,s}, nte_{l,t})$ in Theorem 1 of Appendix A.

$$p^{\text{flow}+}_{l,t,d,s} - B_l \Delta\theta^{+}_{l,t,d,s} \leq 0 \quad \forall l \in \mathcal{L}^{\text{new}}, t, d, s \tag{11}$$

$$p^{\text{flow}-}_{l,t,d,s} - B_l \Delta\theta^{-}_{l,t,d,s} \leq 0 \quad \forall l \in \mathcal{L}^{\text{new}}, t, d, s \tag{12}$$

$$p^{\text{flow}+}_{l,t,d,s} - B_l \Delta\theta^{+}_{l,t,d,s} \geq -M_l(1 - nte_{l,t}) \quad \forall l \in \mathcal{L}^{\text{new}}, t, d, s \tag{13}$$

$$p^{\text{flow}-}_{l,t,d,s} - B_l \Delta\theta^{-}_{l,t,d,s} \geq -M_l(1 - nte_{l,t}) \quad \forall l \in \mathcal{L}^{\text{new}}, t, d, s \tag{14}$$

$$p^{\text{flow}}_{l,t,d,s} = p^{\text{flow}+}_{l,t,d,s} - p^{\text{flow}-}_{l,t,d,s} \quad \forall l \in \mathcal{L}^{\text{new}}, t, d, s \tag{15}$$

$$\theta_{s(l),t,d,s} - \theta_{r(l),t,d,s} = \Delta\theta^{+}_{l,t,d,s} - \Delta\theta^{-}_{l,t,d,s} \quad \forall l \in \mathcal{L}^{\text{new}}, t, d, s \tag{16}$$

$$p^{\text{flow}+}_{l,t,d,s} \leq F^{\max}_l nte_{l,t} \quad \forall l \in \mathcal{L}^{\text{new}}, t, d, s \tag{17}$$

$$p^{\text{flow}-}_{l,t,d,s} \leq F^{\max}_l nte_{l,t} \quad \forall l \in \mathcal{L}^{\text{new}}, t, d, s \tag{18}$$

$$p^{\text{flow}+}_{l,t,d,s}, p^{\text{flow}-}_{l,t,d,s}, \Delta\theta^{+}_{l,t,d,s}, \Delta\theta^{-}_{l,t,d,s} \geq 0 \quad \forall l \in \mathcal{L}^{\text{new}}, t, d, s \tag{19}$$

3.2. Other constraints

All other constraints including operational constraints, investment-related constraints, generator balance constraints, storage constraints, are similar to those of the MILP formulation proposed by Lara et al. [3]. The details of these constraints and the nomenclature can be found in Appendix B.

4. Solution techniques

Given the large size of the proposed GTEP problem, tailored solution approaches need to be developed. In this section, we describe two solution algorithms: a) nested Benders decomposition adapted from [31, 32], which has been used by Lara et al. [3] to solve the GEP model. b) a tailored Benders decomposition. Both of the two algorithms exploit the structure of the GTEP problem.

4.1. Nested Benders decomposition

Lara et al. [3] apply nested Benders decomposition algorithm to solve their GEP model. Like in the GEP model, the nested Benders decomposition algorithm decomposes the fullspace of the GTEP problem by year. Note that the linking constraints for two consecutive years are the investment related constraints. For the investment decisions in transmission lines, the linking constraints are described by equation (1), i.e, the balance of candidate transmission lines. Similarly, there are linking constraints corresponding to the number of thermal generators $ngo^{\text{th}}_{i,r,t}$, the number of renewable generators $ngo^{\text{rn}}_{i,r,t}$, the number of storage units $nso_{j,r,t}$ per region r and year t. These linking constraints can be found in equations (1), and (B.17), (B.20), (B.24) in Appendix B.

From the above observation, variables $nte_{l,t}$, $ngo^{\text{th}}_{i,r,t}$, $ngo^{\text{rn}}_{i,r,t}$, $nso_{j,r,t}$ can be treated as complicating variables. Once these variables are fixed, the GTEP

problem can be decomposed by year. The nested Benders decomposition consists of two phases, i.e., forward pass and backward pass. In the forward pass, the problem is solved sequentially year after year. In each year t, the problem is solved in a myopic way, with the complicating variables of year $t-1$ fixed, and the cutting planes generated from the backward pass. The optimal solution is obtained for year t. Then the complicating variables are fixed for year t and the problem for year $t+1$ is solved, until we reach the end of the planning horizon.

In the backward pass, cutting planes can be generated by solving the LP relaxations of the planning problem with the complicating variables fixed at the values of the forward pass. The backward pass starts from the last year and sequentially adds cutting planes to the previous year. Since the nested Benders decomposition is developed by Lara et al. [3] for the GEP model, we do not provide the details of the algorithms. The steps of the nested Benders algorithms are similar to those in [3], except that in the GTEP problem we introduce new complicating variables $nte_{l,t}$ pertaining to transmission expansion. An additional difference is that while in [3] three different types of cutting planes are implemented in the backward pass, i.e., Benders cuts, strengthened Benders cuts, and Lagrangean cuts, we only implement Benders cuts to solve the GTEP problem because this type of cuts are computationally cheap.

4.2. Tailored Benders decomposition algorithm

Regarding solution technique, the novel contribution of this paper is a tailored Benders decomposition algorithm to solve the GTEP problem. Instead of solving the GTEP problem sequentially by year as in the nested Benders decomposition, we treat all the investment-related variables as complicating variables and include all these variables in a single Benders master problem.

More specifically, the proposed GTEP model can be represented using the succinct form (20) below, where x_t represents all the investment decisions in year t, y_t represents all the operating decisions in the representative days for year t. Note that the investment decisions are made on a yearly basis indexed by t. The operating decisions not only have the index t but also have indices d

and s, which represent the dth representative day in the sth hour, respectively. Since we will decompose the problem by year, we omit the indices d and s and simply use y_t to represent all the operating decisions corresponding to year t. Equations (20c) and (20d) are investment related constraints, which correspond to equations (1), (B.14)-(B.21), (B.23), (B.24). Equations in (20b) describe the operational decisions of each year, such as the power flow equations (2) and (3). Note that equation (20b) can be decomposed by year. Equation (20e) represents the integrality constraints and variable bounds that x_t and y_t have to satisfy.

$$\min \sum_{t \in \mathcal{T}} c_t^T x_t + d_t^T y_t \tag{20a}$$

$$\text{s.t.} \quad A_t x_t + B_t y_t \leq b_t \quad \forall t \in \mathcal{T} \tag{20b}$$

$$C_1 x_1 \leq f_1 \tag{20c}$$

$$C_{t-1} x_{t-1} + D_t x_t \leq f_t \quad t = 2, 3, \ldots, |\mathcal{T}| \tag{20d}$$

$$x_t \in X_t, y_t \in Y_t \quad \forall t \in \mathcal{T} \tag{20e}$$

The GTEP problem has a decomposable structure in the sense that if we treat all the investment decisions x_t for all $t \in \mathcal{T}$ as *complicating variables*, the problem can be decomposed by year. Benders decomposition [33] can be applied to solve this type of problem. We can assign all the investment variables to the Benders master problem and the operating variables y_t to the tth subproblem. After solving the Benders master problem, the investment decisions are fixed and each Benders subproblem can be solved independently. Note that there are some integer variables in the operating decisions, such as the number of generators that are on/off. In order to generate valid Benders cuts, we solve the LP relaxation of each Benders subproblem and add the cuts to the Benders

master problem. A high level description of the algorithm is provided in Figure 2. The formulation of the Benders master problem solved at iteration k is:

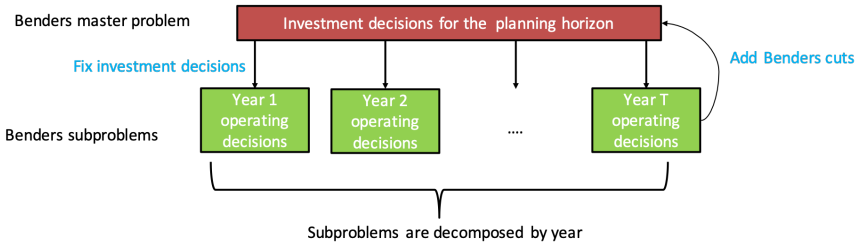

Figure 2: Tailored Benders decomposition algorithm applied to the GTEP problem

$$\min \sum_{t \in \mathcal{T}} c_t^T x_t + \eta_t \tag{21a}$$

$$\text{s.t.} \quad C_1 x_1 \leq f_1 \tag{21b}$$

$$C_{t-1} x_{t-1} + D_t x_t \leq f_t \quad t = 2, 3, \ldots, |\mathcal{T}| \tag{21c}$$

$$\eta_t \geq \tilde{\eta}_t^{k'} + \left(\mu_t^{k'}\right)^T \left(\tilde{x}_t^{k'} - x_t\right) \quad t \in \mathcal{T}, k' < k \tag{21d}$$

$$x_t \in X_t \quad \forall t \in \mathcal{T} \tag{21e}$$

where equation (21d) are the Benders cuts generated by solving the Benders subproblems. We denote the optimal solution of the Benders master problem at iteration k as $\tilde{x}_t^k$, $\forall t \in \mathcal{T}$.

Fixing the values of the investment decision variables to the values obtained at the master problem, i.e., $x_t = \tilde{x}_t^k$, $\forall t \in \mathcal{T}$, we can solve each Benders subproblem independently for each year $t \in \mathcal{T}$:

$$\tilde{\eta}_t^k = \min d_t^T y_t \tag{22a}$$

$$\text{s.t.} \quad x_t = \tilde{x}_t^k \tag{22b}$$

$$A_t x_t + B_t y_t \leq b_t \tag{22c}$$

$$y_t \in \tilde{Y}_t \tag{22d}$$

where all the integer variables in y_t are relaxed and set $\tilde{Y}_t$ represents set Y_t without the integrality constraints, i.e, $\tilde{Y}_t$ only represents variables bounds for y_t. Let μ_t^k be the optimal dual multiplier for equation (22b). A valid Benders cut,

$$\eta_t \geq \tilde{\eta}_t^k + \left(\mu_t^k\right)^T \left(\tilde{x}_t^k - x_t\right)$$

can be generated by solving the tth subproblem. The cuts from the subproblems are then added to the master problem via equation (21d). Note that the Benders subproblem (22) can be infeasible. In this case, a feasibility subproblem should be solved to generate feasibility cuts. Interested readers can refer to [33] for the definitions of feasibility cuts. To simply notation, we assume that the subproblems are feasible here.

At each iteration k, the Benders master problem provides a lower bound of the optimal objective function value with relaxed y_t variables, while an upper bound can be calculated as $\sum_{t\in\mathcal{T}} c_t^T \tilde{x}_t^k + d_t^T \tilde{y}_t^k$ where $\tilde{x}_t^k$ and $\tilde{y}_t^k$ are the optimal solutions to the master problem and the subproblems, respectively. We keep iterating between the Benders master problem (21) and the subproblems (22) until the upper bound and the lower bound overlap.

For our computational study, we use the Benders implementation from CPLEX [34], which is a branch-and-Benders-cut algorithm. We only need to specify the variables in the master problem and the variables in each subproblem and CPLEX automatically solves the GTEP problem using Benders decomposi-

tion. Note that the implementation in CPLEX uses a single branch-and-bound tree where Benders cuts are added as lazy constraints. The Benders subproblems are solved whenever a feasible solution is found in the branch-and-bound tree of the master problem. The corresponding optimality or feasibility cuts will be added to the master problem dynamically in the single branch-and-bound tree.

Since the integrality constraints of the y_t variables are relaxed within the Benders decomposition algorithm, we can only obtain a lower bound to the original GTEP problem (20) through this algorithm. In order to obtain a feasible solution to the original problem, i.e., an upper bound, we can fix the investments decisions x_t to the optimal solution of the Benders decomposition algorithm and solve the operating problem with the integrality constraints of the y_t variables for each year independently. Moreover, as a result of the relaxation of the integrality constraints corresponding to the y_t variables, there will be a gap between the lower bound and the upper bound. However, our computational results in section 5 show that this gap is small. The reason is that all the integer variables in y_t are general integer variables instead of binary variables. Typically, mixed-integer programs with general integer variables have good LP relaxations.

5. Case studies

5.1. Input data

We carry out a GTEP case study for the Electric Reliability Council of Texas (ERCOT). The spatial representation of the ERCOT region has been discussed in subsection 2.4. It is divided into four geographical regions: Northeast, West, Coast and South. Besides these regions, a fifth region, Panhandle, is also included, which is technically outside the ERCOT region, but due to its renewable generation potential, it supplies electricity to the ERCOT regions. Note that in our model, Panhandle is treated as a pure supplier, i.e., it has zero load. The map of the five regions is shown in Figure 1.

Each of the five regions are treated as a bus and a DC power flow model is considered. We specify a city for each region as the location of the bus. The center for Northeast, West, Coast, South and Panhandle are Dallas, Midland, Houston, San Antonio, and Amarillo, respectively. The lengths of the transmission lines are determined by the distance between the centers of any of the two neighboring regions. We assume that all the transmission lines are 500kV lines. To test the GTEP model, we assume that no transmission lines are available, i.e., the model will identify the transmission lines to be built. We assume that for each pair of the two neighboring regions, at most 10 candidate transmission lines can be built. The susceptance and capacity of the transmission lines are all the same, which are obtained from a synthetic grid of Texas [35]. The unit capital cost of transmission lines is obtained from [36].

Old and new generation technologies have been described in subsection 2.1. The investment cost, fixed and variable operating costs for different generation technologies are obtained from the National Renewable Energy Laboratory (NREL), available in the 2016 Annual Technology Baseline (ATB) Spreadsheet [37]. We consider a 20 year time horizon, in which the first year is 2019. The fuel price data for coal, natural gas and uranium correspond to the reference scenario in [38]. A discount rate of 5.7% as chosen in [39] is used. We assume that the carbon tax is zero in the first year and grows linearly across years to \$0.325/kg CO_2.

The hourly solar capacity factor profiles including photo-voltaic (pv) and concentrated solar power (csp), are calculated based on the national solar radiation data base (NSRDB) [40] in 2012 via the System Advisor Model (SAM) [41]. The hourly wind capacity factor profiles are calculated based on the wind speed from the wind integration national dataset (wind) toolkit [42] in 2012 using one power curve from SAM. Since load data are correlated with solar and wind capacity factors, to generate the hourly load profiles we take load data from ERCOT in 2012 and scale them so that the annual load for each ERCOT region is equal to the annual load in 2019. To sum up, we have 365 days (the leap day is excluded) of 24 hour solar and wind capacity factor and load data.

To select the representative days for the GTEP model, we use the software package, TimeSeriesClustering.jl developed by Teichgraeber and Brandt [28]. By using this package, we are able to apply the k-means clustering algorithm to the time series and select the centroid of each cluster as the representative day. The details of the clustering algorithms are described in [28]. The capacity factors are assumed to be unchanged over the planning horizon. The annual load growth rate is assumed to be 1.4%.

5.2. Comparison of formulations and algorithms

All the MILP formulations are implemented in Pyomo/Python [43]. We first solve the GTEP model directly with CPLEX 12.9.0.0. We compare the three transmission expansion formulations proposed in subsection 3.1. All the problems in this paper are solved using one processor of an Intel Xeon (2.67GHz) machine with 64 GB RAM. The time limit is set to 10 hours. The number of general integer variables, binary variables, continuous variables, and constraints of the fullspace GTEP problem with the three different formulations are shown in Table 1. The upper bound (UB), lower bound (LB) of the optimal value of the objective function in billion dollars and the wall time in seconds are also shown in Table 1. All the three formulations have the same number of general integer variables and binary variables but differ in the number of continuous variables. The standard big-M formulation uses the fewest number of continuous variables and constraints. CPLEX is not able to find a feasible solution (UB) for any of the three formulations within the prespecified time limit. The lower bound column (LB) provides the bound that CPLEX returns at termination. In fact, we direct CPLEX to solve the LP relaxation for each of the three formulations, but CPLEX was not able to return a solution for any of the formulations within the 10-hour time limit, regardless of the LP algorithm chosen.

We also test the two decomposition algorithms described in section 4. The nested Benders decomposition is implemented in Pyomo/Python [43]. The tailored Benders decomposition implementation is from CPLEX [34], which is called using the Pyomo persistent solver interface [44]. The computational re-

Table 1: Computational statistics for the fullspace problem with 4 representative days

Formulation	Int Var	Bin Var	Cont Var	Constraints	UB ($10^9)	LB ($10^9)	Wall time (sec)
big-M	274,920	2,800	564,826	1,543,966	-	21.13	36,000
alternative big-M	274,920	2,800	1,102,426	2,081,566	-	21.13	36,000
hull	274,920	2,800	833,626	2,081,566	-	281.73	36,000

sults of the two proposed decomposition algorithms are shown in Table 2.

The tailored Benders decomposition algorithm is able to solve all the three formulations to within 1% optimality gap within 10,000 seconds.

For the nested Benders decomposition, we observe that the forward pass with integrality constraints is expensive to solve. Therefore, we make a change in the implementation so that we first use the nested Benders decomposition algorithm to solve the LP relaxation of the problem until the LP relaxation is solved to optimality or we reach the time limit of 10 hours or the iteration limit of 100. Then we perform one single forward pass with the integrality constraints to obtain a feasible solution. Although the nested Benders decomposition can obtain an upper bound and a lower bound to all the three formulations, the optimality gaps are large compared to the results from the tailored Benders decomposition. In fact, in none of the three formulations is the nested Benders decomposition able to solve the LP relaxation of the problems to optimality within the time limit. Note that the performance of the nested Benders decomposition is quite different from the numerical experiments on the GEP model performed by Lara et al. [3] for the GEP model where the nested Benders decomposition performs well. The reason for this difference could be due to the complication brought by the transmission expansion constraints and the DC power flow equations of the GTEP model. As a result, the subproblems become larger and more dual degenerate, which makes nested Benders decomposition take not only more time to solve each iteration but also more iterations to converge.

From this numerical experiment, the tailored Benders decomposition algorithm with the alternative big-M formulation proves to be the fastest. We adopt this algorithm-formulation combination for the rest of the experiments in this paper.

Table 2: Computational results of the two proposed decomposition algorithms using different formulations

Algorithm	Formulation	UB ($\$10^9$)	LB ($\$10^9$)	Gap	Wall time (secs)
tailored Benders	big-M	283.7	282.6	0.38%	5,115
tailored Benders	alternative big-M	283.9	281.6	0.82%	3,693
tailored Benders	hull	282.6	280.6	0.71%	8,418
nested Benders	big-M	295.7	268.9	9.98%	53,682
nested Benders	alternative big-M	294.2	265.5	10.81%	43,389
nested Benders	hull	288.0	269.3	6.97%	37,577

5.3. Results with 15 representative days

We improve the fidelity of the model by increasing the number of representative days to 15. The 15 representative day model with the alternative big-M formulation has 2,800 binary variables, 1,024,680 general integer variables, 4,120,606 continuous variables, and 7,787,266 constraints. The proposed tailored Benders decomposition algorithm is able to solve the problem in 33,207 seconds with an upper bound of 301.1 ($\$10^9$), a lower bound of 299.9 ($\$10^9$) and an optimality gap of 0.4%.

The capacities of different generation technologies from 2019 to 2038 are shown in Figure 3. The results include high capacities of solar and wind. The aggregated natural gas capacity of the five regions increases in the first few years, reaches its peak in 2024 and gradually decreases afterwards due to the retirement of old generators and the increase in carbon tax, which makes the natural gas generators less competitive compared with solar and wind generators. The nuclear and coal capacities are unchanged throughout the planning horizon. No storage unit is installed.

Geographically, most of the solar and wind capacity additions are projected to take place in the West and Panhandle regions because the capacity factors for solar and wind are higher in these two regions. The projected capacity for natural gas in the four regions, i.e., Coast, Northeast, South, and West, are shown in Figure 4. It can be seen that most natural gas expansions are expected to take place in the Northeast and Coast regions where the absolute increase in load is high and capacity factors for renewables are relatively low. In the

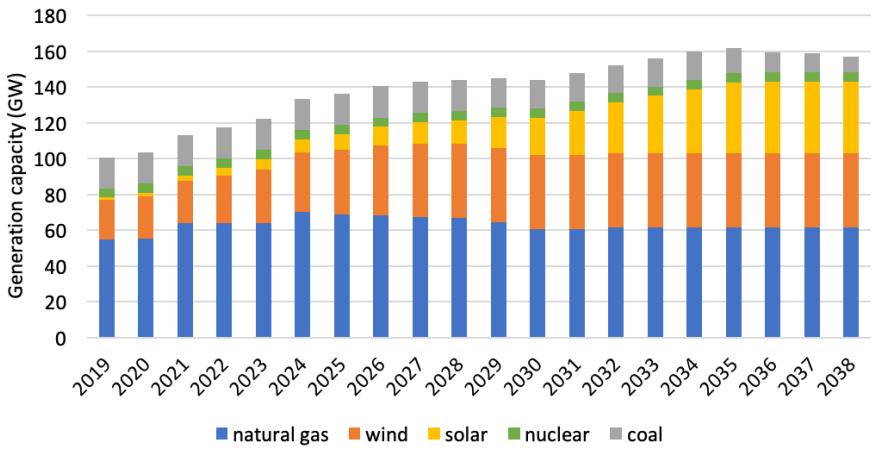

Figure 3: Aggregated generation expansion results

West region, where the absolute load increase is low and the capacity factors for renewable generation are high, we observe very marginal changes in natural gas capacity. In the South region, natural gas capacity increases in the first few years and reaches a peak in 2025. After 2025, natural gas capacity decreases over the years due to the retirement of old generators. The load growth in South is satisfied by power transfers from West region, which we analyze below.

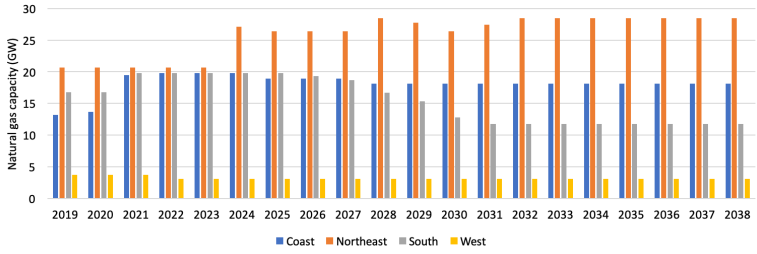

Figure 4: Projected capacity expansions for natural gas in Coast, Northeast, South, and West

The number of transmission lines built over the planning horizon are shown in Figure 5. Most of the transmission lines are built for Northeast-Panhandle and South-West in order to transfer the power generated by the renewable sources in West and Panhandle to other regions. Note that we assume that no

transmission lines are built *a priori*. The transmission expansion results from our model coincide with what has happened in practice, since transmission lines have been built from the remote West part of Texas to the more populous regions in the South and the East. It is clear that there are correlations between the geographical locations of the generation technologies and the transmission expansion decisions.

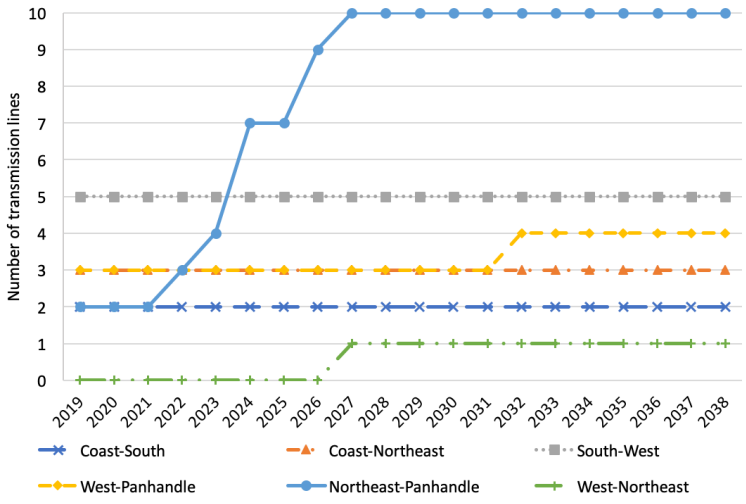

Figure 5: Transmission expansion results

Figure 6 shows the aggregated power flow through all the installed transmission lines at a peak load time period ($t = 20$, $d = 15$, $s = 24$). The directions and the magnitudes of the power flows are represented by the red arrows and numbers in this Figure. The most significant power flows are from Panhandle to Northeast and from West to South due the surplus of their renewable energy generation.

5.4. Sensitivity analysis of input generator data

The generation capacity expansion planning results can be sensitive to the forecast of future capital cost and operating cost of the potential generating units. Recall that generator cost data for the previous analysis are from the National Renewable Energy Laboratory (NREL), available in the 2016 Annual

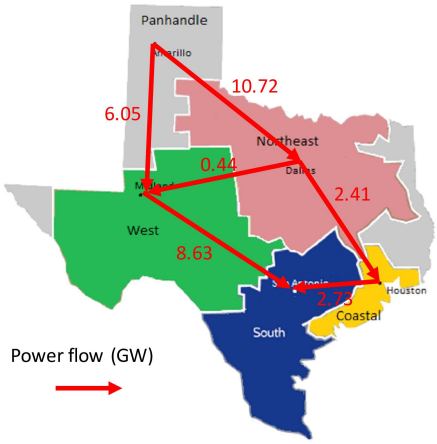

Figure 6: Aggregated power flow directions and magnitudes for all the transmission lines at $t = 20$, $d = 15$, $s = 24$

Technology Baseline (ATB) Spreadsheet [37]. We switch the capital cost and operating cost data for all the generators to internal data from IHS Markit and re-run the Benders decomposition experiment with 15 representative days. The proposed tailored Benders decomposition algorithm is able to solve the problem in 51,445 seconds with an upper bound of 294.4 ($\$10^9$), a lower bound of 293.7 ($\$10^9$) and an optimality gap of 0.2%. The increase in computational time compared with using NREL data is 67%.

The generation expansion results are shown in Figure 7. The major change is that the IHS Markit results favors more wind and less solar compared with the results shown in Figure 3. To give some insight on why this happens, we find that the overnight cost of the wind generating units in the IHS Markit dataset is 25% lower than that in the NREL dataset in the first year of the planning horizon. Whereas, the overnight cost for the PV generating units is only 11% lower in the first year. We demonstrate that the change in the forecast for generator cost can change the final generation expansion planning results. Therefore, having a good forecast of the capital and operating cost is essential in making the capacity expansion decisions.

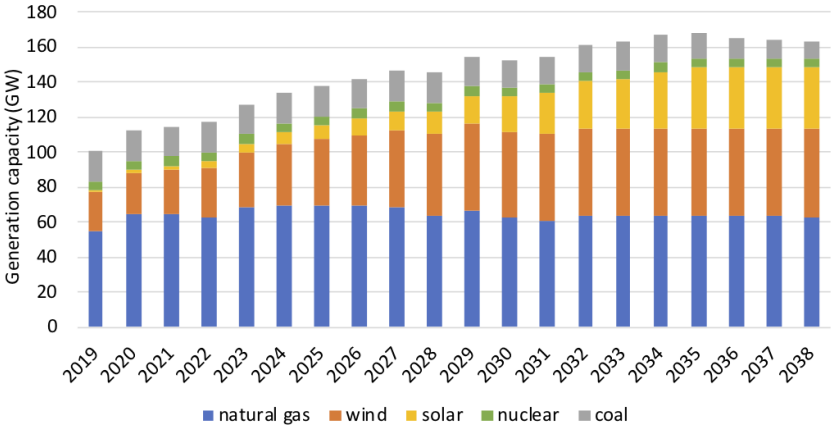

Figure 7: Generation expansion results using generating unit cost data from IHS Markit

6. Conclusions

In this paper, we address generation and transmission expansion planning (GTEP) problem by developing MILP formulations and solution techniques. We consider both thermal and renewable technologies as expansion candidates. Operating and transmission constraints are included in the model, which leads to large scale problems. To limit the size of the GTEP model, several simplifications are made. We aggregate the generators that use the same technology assuming that they have the same design parameters. We also spatially aggregate regions with similar climate and load profiles. For example, the ERCOT is divided into five regions. Each region represents one bus in the power flow model. Therefore, we only consider the expansion of tielines between regions. In terms of temporal representation, we select some representative days with hourly load and capacity factor data. The representative days are selected by a clustering algorithm such as k-means clustering.

The model is a multi-scale MILP model with both investment decisions and operating decisions. We compare three different formulations for transmission expansion, i.e., the big-M formulation, the hull formulation and the alternative big-M formulation. We prove that the alternative big-M (ABM) formulation has

the same feasible region as the big-M formulation (BM) when projected onto the space of the variables involved in the big-M formulation. Computational experiments are performed as well for the three formulations, but it is hard to identify a clear winner among the three formulations.

Two solution techniques, a nested Benders decomposition algorithm and a tailored Benders decomposition algorithm, are proposed. Both algorithms decompose the planning problem by year. The nested Benders decomposition solves each year sequentially in a forward and backward pass manner. The Benders decomposition defines a master problem that deals with the investment decisions and a number of subproblems corresponding to representative operating decisions for a given year. The tailored Benders decomposition algorithm outperforms the nested Benders decomposition one in our computational experiments.

An ERCOT case study is used to demonstrate the GTEP model and the solution techniques. The tailored Benders decomposition is able to solve the 20 year planning problem with 15 representative days. The capacity expansion mix for ERCOT will mainly include solar and wind capacities in the West and Panhandle regions. The transmission lines are mainly built to transfer power from solar and wind rich regions to the South and Northeast regions of ERCOT, which shows that the generation and transmission decisions are correlated. Co-optimization of generation and transmission has the potential of bring additional value to the system operator/regulator than solving the two planning problems independently.

Future work will be focused on considering uncertainties in the GTEP model by using a multi-stage stochastic programming framework. It is also worth testing the model in a different ISO that with a diversity of geographical regions.

Appendix A

Theorem 1. *The alternative big-M formulation (*ABM) has the same feasible region as the big-M (BM) formulation if the feasible region of ABM is projected to the space of $\Big\{ \underset{l\in\mathcal{L}^{\text{new}},t\in\mathcal{T},d\in\mathcal{D},s\in\mathcal{S}}{\oplus} (p^{\text{flow}}_{l,t,d,s}, \theta_{s(l),t,d,s}, \theta_{r(l),t,d,s}, nte_{l,t}) \Big\}$, where the symbol '$\oplus$' means the concatenation of all the variables $(p^{\text{flow}}_{l,t,d,s}, \theta_{s(l),t,d,s}, \theta_{r(l),t,d,s}, nte_{l,t})$ over the set $\mathcal{L}^{\text{new}}, \mathcal{T}, \mathcal{D}, \mathcal{S}$.

Proof. We first denote the feasible region of ABM as,

$$\mathcal{F}_{\text{ABM}} \coloneqq \Big\{ \underset{l\in\mathcal{L}^{\text{new}},t\in\mathcal{T},d\in\mathcal{D},s\in\mathcal{S}}{\oplus} \big(p^{\text{flow}}_{l,t,d,s}, p^{\text{flow}+}_{l,t,d,s}, p^{\text{flow}-}_{l,t,d,s}, \theta_{s(l),t,d,s}, \theta_{r(l),t,d,s}, \Delta\theta^{+}_{l,t,d,s}, \Delta\theta^{-}_{l,t,d,s}, nte_{l,t}\big) \Big| (11)-(18) \Big\}$$

and the feasible region of BM as

$$\mathcal{F}_{\text{BM}} \coloneqq \Big\{ \underset{l\in\mathcal{L}^{\text{new}},t\in\mathcal{T},d\in\mathcal{D},s\in\mathcal{S}}{\oplus} \big(p^{\text{flow}}_{l,t,d,s}, \theta_{s(l),t,d,s}, \theta_{r(l),t,d,s}, nte_{l,t}\big) \Big| (5), (6) \Big\}$$

To simplify notation, we drop the concatenation symbol '$\underset{l\in\mathcal{L}^{\text{new}},t\in\mathcal{T},d\in\mathcal{D},s\in\mathcal{S}}{\oplus}$' hereafter in the proof. the projection of $\mathcal{F}_{\text{ABM}}$ onto the space of $(p^{\text{flow}}_{l,t,d,s}, \theta_{s(l),t,d,s}, \theta_{r(l),t,d,s}, nte_{l,t})$ is denoted as $\text{Proj}(\mathcal{F}_{\text{ABM}})$. We want to prove that $\text{Proj}(\mathcal{F}_{\text{ABM}}) = \mathcal{F}_{\text{BM}}$.
We first prove that $\mathcal{F}_{\text{BM}} \subseteq \text{Proj}(\mathcal{F}_{\text{ABM}})$. It suffices to prove that for any $\big(p^{\text{flow},0}_{l,t,d,s}, \theta^{0}_{s(l),t,d,s}, \theta^{0}_{r(l),t,d,s}, nte^{0}_{l,t}\big) \in \mathcal{F}_{\text{BM}}$. We can always find $p^{\text{flow}+,0}_{l,t,d,s}$, $p^{\text{flow}-,0}_{l,t,d,s}$, $\Delta\theta^{+,0}_{l,t,d,s}$, $\Delta\theta^{-,0}_{l,t,d,s}$, such that

$$\big(p^{\text{flow},0}_{l,t,d,s}, p^{\text{flow}+,0}_{l,t,d,s}, p^{\text{flow}-,0}_{l,t,d,s}, \theta^{0}_{s(l),t,d,s}, \theta^{0}_{r(l),t,d,s}, \Delta\theta^{+,0}_{l,t,d,s}, \Delta\theta^{-,0}_{l,t,d,s}, nte^{0}_{l,t}\big) \in \mathcal{F}_{\text{ABM}}$$

It is easy to check that by setting,

$$\begin{aligned}
p^{\text{flow}+,0}_{l,t,d,s} &= \max\big(0, p^{\text{flow},0}_{l,t,d,s}\big) \\
p^{\text{flow}-,0}_{l,t,d,s} &= \max\big(0, -p^{\text{flow},0}_{l,t,d,s}\big) \\
\Delta\theta^{+,0}_{l,t,d,s} &= \max\big(0, \theta^{0}_{s(l),t,d,s} - \theta^{0}_{r(l),t,d,s}\big) \\
\Delta\theta^{-,0}_{l,t,d,s} &= \max\big(0, \theta^{0}_{r(l),t,d,s} - \theta^{0}_{s(l),t,d,s}\big)
\end{aligned}$$

for all $l \in \mathcal{L}^{\text{new}}, t \in \mathcal{T}, d \in \mathcal{D}, s \in \mathcal{S}$, constraints (11)-(18) can be satisfied.

Next, we prove that $\text{Proj}(\mathcal{F}_{\text{ABM}}) \subseteq \mathcal{F}_{\text{BM}}$. It suffices to show that equations (5) and (6) are consequences of equations (11)-(18) by carefully choosing Farkas multipliers. For example, inequality $p^{\text{flow}}_{l,t,d,s} - B_l(\theta_{s(l),t,d,s} - \theta_{r(l),t,d,s}) \leq M_l(1 - nte_{l,t})$ can be obtained by (11) − (14) + (15) − $B_l \times$ (16). Inequality $p^{\text{flow}}_{l,t,d,s} \leq F^{\max}_l nte_{l,t}$ can be obtained by (15)+(17)+$[-p^{\text{flow}-,0}_{l,t,d,s} \leq 0]$. The other two inequalities in equations (5) and (6) can be obtained similarly. We conclude $\text{Proj}(\mathcal{F}_{\text{ABM}}) \subseteq \mathcal{F}_{\text{BM}}$. □

Appendix B

Nomenclature

Indices and Sets

$r \in \mathcal{R}$	set of regions within the area considered
$i \in \mathcal{I}$	set of generator clusters
$i \in \mathcal{I}_r$	set of generator clusters in region r
$i \in \mathcal{I}^{\text{old}}_r$	set of existing generator clusters in region r at the beginning of the time horizon, $\mathcal{I}^{\text{old}}_r \subseteq \mathcal{I}_r$
$i \in \mathcal{I}^{\text{new}}_r$	set of potential generator clusters in region r, $\mathcal{I}^{\text{new}}_r \subseteq \mathcal{I}_r$
$i \in \mathcal{I}^{\text{TH}}_r$	set of thermal generator clusters in region r, $\mathcal{I}^{\text{TH}}_r \subseteq \mathcal{I}_r$
$i \in \mathcal{I}^{\text{RN}}_r$	set of renewable generator clusters in region r, $\mathcal{I}^{\text{RN}}_r \subseteq \mathcal{I}_r$
$i \in \mathcal{I}^{\text{Told}}_r$	set of existing thermal generator clusters in region r, $\mathcal{I}^{\text{Told}}_r \subseteq \mathcal{I}^{\text{TH}}_r$
$i \in \mathcal{I}^{\text{Tnew}}_r$	set of potential thermal generator clusters in region r, $\mathcal{I}^{\text{Tnew}}_r \subseteq \mathcal{I}^{\text{TH}}_r$
$i \in \mathcal{I}^{\text{Rold}}_r$	set of existing renewable generator clusters in region r, $\mathcal{I}^{\text{Rold}}_r \subseteq \mathcal{I}^{\text{RN}}_r$
$i \in \mathcal{I}^{\text{Rnew}}_r$	set of potential renewable generator clusters in region r, $\mathcal{I}^{\text{Rnew}}_r \subseteq \mathcal{I}^{\text{RN}}_r$
$l \in \mathcal{L}^{\text{old}}$	set of existing transmission lines
$l \in \mathcal{L}^{\text{new}}$	set of prospective transmission lines
$j \in \mathcal{J}$	set of storage unit clusters
$t \in \mathcal{T}$	set of time periods (years) within the planning horizon
$d \in \mathcal{D}$	set of representative days in each year t
$s \in \mathcal{S}$	set of sub-periods of time per representative day d in year t
$k \in \mathcal{K}$	set of iterations in the Nested Decomposition algorithm

Deterministic Parameters

$L_{r,t,d,s}$	load demand in region r in sub-period s of representative day d of year t (MW)
$L^{\max}_t$	peak load in year t (MW)
W_d	weight of the representative day d
Hs	duration of sub-period s (hours)
$Qg^{\text{np}}_{i,r}$	nameplate (nominal) capacity of a generator in cluster i in region r (MW)

$Ng_{i,r}^{\text{old}}$	number of existing generators in each cluster, $i \in \mathcal{I}_r^{\text{old}}$, per region r at the beginning of the time horizon
Nt_l^{old}	number of units of existing transmission lines for line l
$Ng_i^{\max}$	maximum number of generators in the potential clusters $i \in \mathcal{I}_r^{\text{new}}$
$Q_{i,t}^{\text{inst,UB}}$	upper bound on yearly capacity installations based on generation technology ($^{\text{MW}}/_{\text{year}}$)
$R_t^{\min}$	system's minimum reserve margin for year t (fraction of the peak load)
ED_t	energy demand during year t (MWh)
LT_i	expected lifetime of generation cluster i (years)
T_t^{remain}	remaining time until the end of the time horizon at year t (years)
$Ng_{i,r,t}^{\text{r}}$	number of generators in cluster i of region r that achieved their expected lifetime
Q_i^{v}	capacity value of generation cluster i (fraction of the nameplate capacity)
$Cf_{i,r,t,d,s}$	capacity factor of generation cluster $i \in \mathcal{I}_r^{\text{RN}}$ in region r at sub-period s, of representative day d of year t (fraction of the nameplate capacity)
$Pg_i^{\min}$	minimum operating output of a generator in cluster $i \in \mathcal{I}_r^{\text{TH}}$ (fraction of the nameplate capacity)
$Ru_i^{\max}$	maximum ramp-up rate for cluster $i \in \mathcal{I}_r^{\text{TH}}$ (fraction of nameplate capacity)
$Rd_i^{\max}$	maximum ramp-down rate for cluster $i \in \mathcal{I}_r^{\text{TH}}$ (fraction of nameplate capacity)
F_i^{start}	fuel usage at startup (MMbtu/MW)
$Frac_i^{\text{spin}}$	maximum fraction of nameplate capacity of each generator that can contribute to spinning reserves (fraction of nameplate capacity)
$Frac_i^{\text{Qstart}}$	maximum fraction of nameplate capacity of each generator that can contribute to quick-start reserves (fraction of nameplate capacity)
$Op^{\min}$	minimum total operating reserve (fraction of the load demand)
$Spin^{\min}$	minimum spinning operating reserve (fraction of the load demand)
$Qstart^{\min}$	minimum quick-start operating reserve (fraction of the load demand)
α^{RN}	fraction of the renewable generation output covered by quick-start reserve (fraction of total renewable power output)
B_l	susceptance of transmission line l
$F_l^{\max}$	capacity of transmission line l (MW)
$TIC_{l,t}$	discounted investment cost of transmission line l in year t
$Ns_{j,r}$	number of existing storage units in each cluster j per region r at the beginning of the time horizon
$Charge_j^{\min}$	minimum operating charge for storage unit in cluster j (MW)
$Charge_j^{\max}$	maximum operating charge for storage unit in cluster j (MW)
$Discharge_j^{\min}$	minimum operating discharge for storage unit in cluster j (MW)
$Discharge_j^{\max}$	maximum operating discharge for storage unit in cluster j (MW)
$Storage_j^{\min}$	minimum storage capacity for storage unit in cluster j (MWh)
$Storage_j^{\max}$	maximum storage capacity (i.e. nameplate capacity) for storage unit in cluster j (MWh)
η_j^{charge}	charging efficiency of storage unit in cluster j (fraction)
$\eta_j^{\text{discharge}}$	discharging efficiency of storage unit in cluster j (fraction)
LT_j^{s}	lifetime of storage unit in cluster j (years)
Ir	nominal interest rate
If_t	discount factor for year t
$OCC_{i,t}$	overnight capital cost of generator cluster i in year t ($^{\$}/_{\text{MW}}$)
$ACC_{i,t}$	annualized capital cost of generator cluster i in year t ($^{\$}/_{\text{MW}}$)

$DIC_{i,t}$	discounted investment cost of generator cluster i in year t ($/MW) [1]
$SIC_{j,t}$	investment cost of storage cluster j in year t ($/MW)
CC_i^{m}	capital cost multiplier of generator cluster i (unitless)
LE_i	life extension cost for generator cluster i (fraction of the investment cost of corresponding new generator)
$FOC_{i,t}$	fixed operating cost of generator cluster i ($/MW)
$P_{i,t}^{\mathrm{fuel}}$	price of fuel for generator cluster i in year t ($/MMBtu)
HR_i	heat rate of generator cluster i (MMBtu/MWh)
$Tx_t^{\mathrm{CO_2}}$	carbon tax in year t ($/kg CO_2)
$EF_i^{\mathrm{CO_2}}$	full lifecycle CO_2 emission factor for generator cluster i ($kgCO_2$/MMBtu)
$VOC_{i,t}$	variable O&M cost of generator cluster i ($/MWh)
RN_t^{min}	minimum renewable energy production requirement during year t (fraction of annual energy demand)
PEN_t^{rn}	penalty for not meeting renewable energy quota target during year t ($/MWh)
PEN_t^{c}	penalty for curtailment during year t ($/MWh)
C_i^{start}	fixed startup cost for generator cluster i ($/MW)
M_l	big-M parameter for line l in transmission expansion equations
$s(l)$	sending end of transmission line l
$r(l)$	receiving end of transmission line l

Continuous variables

Φ	net present cost throughout the time horizon, including amortized investment cost, operational and environmental cost ($)
Φ_t^{opex}	amortized operating costs in year t ($)
Φ_t^{capex}	amortized investment costs in year t ($)
Φ_t^{PEN}	amortized penalty costs in year t ($)
$p_{i,r,t,d,s}$	power output of generation cluster i in region r during sub-period s of representative day d of year t (MW)
def_t^{rn}	deficit from renewable energy quota target during year t (MWh)
$cu_{r,t,ss,s}$	curtailment slack generation in region r during sub-period s of representative day d of year t (MW)
$p_{l,t,d,s}^{\mathrm{flow}}$	power transfer through transmission line l during sub-period s of representative day d of year t (MW)
$p_{l,t,d,s}^{\mathrm{flow+}}$	nonnegative variable, power flow from the sending end of transmission line l, $s(l)$, to the receiving end of line l, $r(l)$ during sub-period s of representative day d of year t (MW)
$p_{l,t,d,s}^{\mathrm{flow-}}$	nonnegative variable, power flow from the receiving end of transmission line l, $r(l)$, to the sending end of line l, $s(l)$ during sub-period s of representative day d of year t (MW)
$\theta_{r,t,d,s}$	voltage angle at region r during sub-period s of representative day d of year t
$\theta_{s(l),t,d,s}$	voltage angle at sending end of transmission line l during sub-period s of representative day d of year t

[1] $DIC_{i,t}$ is used in the calculation for the life extension investment cost, which is in terms of a fraction LE_i of the capital cost. Therefore the investment cost for the existing cluster is approximated as being the same as for the potential clusters that have the same or similar generation technology.

$\theta_{r(l),t,d,s}$	voltage angle at receiving end of transmission line l during sub-period s of representative day d of year t
$\Delta\theta^1_{l,t,d,s}$	disaggregated variable in the hull formulation, angle difference between the angles at sending end and receiving end of transmission line l during sub-period s of representative day d of year t (MW) if the transmission line l exists in year t
$\Delta\theta^2_{l,t,d,s}$	disaggregated variable in the hull formulation, angle difference between the angles at sending end and receiving end of transmission line l during sub-period s of representative day d of year t (MW) if the transmission line l does not exist in year t
$\Delta\theta^+_{l,t,d,s}$	nonnegative variable, angle difference between the angles at sending end and receiving end of transmission line l during sub-period s of representative day d of year t (MW)
$\Delta\theta^-_{l,t,d,s}$	nonnegative variable, angle difference between the angles at receiving end and sending end of transmission line l during sub-period s of representative day d of year t (MW)
$q^{\text{spin}}_{i,r,t,d,s}$	spinning reserve capacity of generation cluster i in region r during sub-period s of representative day d of year t (MW)
$q^{\text{Qstart}}_{i,r,t,d,s}$	quick-start capacity reserve of generation cluster i in region r during sub-period s of representative day d of year t (MW)
$ngo^{\text{rn}}_{i,r,t}$	number of generators that are operational in cluster $i \in \mathcal{I}^{\text{RN}}_r$ of region r in year t (continuous relaxation)
$ngb^{\text{rn}}_{i,r,t}$	number of generators that are built in cluster $i \in \mathcal{I}^{\text{RN}}_r$ of region r in year t (continuous relaxation)
$ngr^{\text{rn}}_{i,r,t}$	number of generators that retire in cluster $i \in \mathcal{I}^{\text{RN}}_r$ of region r in year t (continuous relaxation)
$nge^{\text{rn}}_{i,r,t}$	number of generators that had their life extended in cluster $i \in \mathcal{I}^{\text{RN}}_r$ of region r in year t (continuous relaxation)
$p^{\text{charge}}_{j,r,t,d,s}$	power being charged to storage cluster j is region r, during sub-period s of representative day d of year t (MW)
$p^{\text{discharge}}_{j,r,t,d,s}$	power being discharged to storage cluster j is region r, during sub-period s of representative day d of year t (MW)
$p^{\text{level}}_{j,r,t,d,s}$	state of charge of storage cluster j is region r, during sub-period s of representative day d of year t (MWh)
$p^{\text{level,0}}_{j,r,t,d}$	state of charge of storage cluster j is region r at hour zero of representative day d of year t (MWh)
$nso_{j,r,t}$	number of storage units that are operational in cluster j of region r in year t (continuous relaxation)
$nsb_{j,r,t}$	number of storage units that are built in cluster j of region r in year t (continuous relaxation)
$nsr_{j,r,t}$	number of storage units that retire in cluster j of region r in year t (continuous relaxation)
Φ_t	objective function value for subproblem t assuming exact representation of the cost-to-go function (\$)
$\Phi_{t,k}$	objective function value for subproblem t in iteration k (\$)
$\phi_{t,k}$	cost-to-go function (\$)
α_t	expected future year cost, when calculating the cost for year t (\$)
$\Phi^{\text{LP}}_{t,k}$	net present cost of the linear relaxation of the subproblem for year t in iteration k (\$)
$\Phi^{\text{LR}}_{t,k}$	net present cost of the Lagrangean relaxation of the subproblem for year t in iteration k (\$)
$\Phi^{\text{LD}}_{t,k}$	net present cost of the Lagrangean dual of the subproblem for year t in iteration k (\$)
$\Phi^{\text{OP}}_{t,k}$	net present cost of the original MILP subproblem for year t in iteration k (\$)

$ngo^{\mathrm{rn,prev}}_{i,r,t}$	number of generators that are operational in cluster $i \in \mathcal{I}^{\mathrm{RN}}_r$ of region r in year $t-1$ (continuous relaxation)
$ngb^{\mathrm{rn,LT}}_{i,r,t}$	number of generators that are built in cluster $i \in \mathcal{I}^{\mathrm{RN}}_r$ of region r in year $t - LT_i$ (continuous relaxation)
$ngo^{\mathrm{th,prev}}_{i,r,t}$	number of generators that are operational in cluster $i \in \mathcal{I}^{\mathrm{TH}}_r$ of region r in year $t-1$ (continuous relaxation)
$ngb^{\mathrm{th,prev}}_{i,r,t}$	number of generators that are built in cluster $i \in \mathcal{I}^{\mathrm{TH}}_r$ of region r in year $t - LT_i$ (continuous relaxation)
x_t	investment variables in year t in the concise notation
y_t	operating variables in year t in the concise notation

Discrete variables

$ngo^{\mathrm{th}}_{i,r,t}$	number of generators that are operational in cluster $i \in \mathcal{I}^{\mathrm{TH}}_r$ of region r in year t (integer variable)
$ngb^{\mathrm{th}}_{i,r,t}$	number of generators that are built in cluster $i \in \mathcal{I}^{\mathrm{TH}}_r$ of region r in year t (integer variable)
$ngr^{\mathrm{th}}_{i,r,t}$	number of generators that retire in cluster $i \in \mathcal{I}^{\mathrm{TH}}_r$ of region r in year t (integer variable)
$nge^{\mathrm{th}}_{i,r,t}$	number of generators that had their life extended in cluster $i \in \mathcal{I}^{\mathrm{TH}}_r$ of region r in year t (integer variable)
$ntb_{l,t}$	binary variable, to denote whether transmission line l is built in year t or not
$nte_{l,t}$	binary variable, represents whether transmission line l has been installed in year t
$u_{i,r,t,d,s}$	number of thermal generators ON in cluster $i \in \mathcal{I}_r$ of region r during sub-period s of representative day d of year t (integer variable)
$su_{i,r,t,d,s}$	number of generators starting up in cluster i during sub-period s of representative day d in year t (integer variable)
$sd_{i,r,t,d,s}$	number of generators shutting down in cluster i during sub-period s of representative day d in year t (integer variable)

B.1 Operational constraints

The energy balance (B.1) ensures that, in each sub-period s of representative day d in year t, the sum of instantaneous power $p_{i,r,t,d,s}$ generated by generator clusters i in region r, plus the power flows through the transmission lines l whose receiving end is region r, $\sum_{l|r(l)=r} p^{\mathrm{flow}}_{l,t,d,s}$, minus the power flows through the transmission lines l whose sending end is region r, $\sum_{l|s(l)=r} p^{\mathrm{flow}}_{l,t,d,s}$, plus the power discharged from all the storage clusters j in region r, $p^{\mathrm{discharge}}_{j,r,t,d,s}$, equals the load demand $L_{r,t,d,s}$ at that region r, plus the power being charged to the storage clusters j in region r, $p^{\mathrm{charge}}_{j,r,t,d,s}$, plus a slack for curtailment of renewable generation $cu_{r,t,d,s}$. Note that we have specified the directions of the

transmission lines. Therefore, the signs of the power flows are unrestricted.

$$\sum_{i}(p_{i,r,t,d,s}) + \sum_{l|r(l)=r} p^{\text{flow}}_{l,t,d,s} - \sum_{l|s(l)=r} p^{\text{flow}}_{l,t,d,s} + \sum_{j} p^{\text{discharge}}_{j,r,t,d,s} = L_{r,t,d,s} + \sum_{j} p^{\text{charge}}_{j,r,t,d,s} + cu_{r,t,d,s} \quad \forall\, r,t,d,s \tag{B.1}$$

The capacity factor constraint (B.2) limits the power outlet $p_{i,r,t,d,s}$ of renewable generators to be equal to a fraction $Cf_{i,r,t,d,s}$ of the nameplate capacity $Qg^{\text{np}}_{i,r}$ in each sub-period s of representative day d in year t, where $ngo^{\text{rn}}_{i,r,t}$ represents the number of renewable generators that are operational in year t. Due to the flexibility in sizes for renewable generators, $ngo^{\text{rn}}_{i,r,t}$ is relaxed to be continuous.

$$p_{i,r,t,d,s} = Qg^{\text{np}}_{i,r} \cdot Cf_{i,r,t,d,s} \cdot ngo^{\text{rn}}_{i,r,t} \qquad \forall\, i \in \mathcal{I}^{\text{RN}}_{r}, r,t,d,s \tag{B.2}$$

The unit commitment constraint (B.3) computes the number of generators that are ON, $u_{i,r,t,d,s}$, or in startup, $su_{i,r,t,d,s}$, and shutdown, $sd_{i,r,t,d,s}$, modes in cluster i in sub-period s of representative day d of year t, and treated as integer variables.

$$u_{i,r,t,d,s} = u_{i,r,t,d,s-1} + su_{i,r,t,d,s} - sd_{i,r,t,d,s} \quad \forall\, i \in \mathcal{I}^{\text{TH}}_{r}, r,t,d,s \tag{B.3}$$

The ramping limit constraints (B.4)-(B.5) capture the limitation on how fast thermal units can adjust their output power, $p_{i,r,t,d,s}$, where $Ru^{\max}_{i}$ is the maximum ramp-up rate, $Rd^{\max}_{i}$ is the maximum ramp-down rate, and $Pg^{\min}_{i}$ is the

minimum operating limit.

$$p_{i,r,t,d,s} - p_{i,r,t,d,s-1} \leq \quad Ru_i^{\max} \cdot Hs \cdot Qg_{i,r}^{\text{np}} \cdot (u_{i,r,t,d,s} - su_{i,r,t,d,s}) + \max\left(Pg_i^{\min}, Ru_i^{\max} \cdot Hs\right) \cdot Qg_{i,r}^{\text{np}} \cdot su_{i,r,t,d,s} \quad \forall\ i \in \mathcal{I}_r^{\text{TH}}, r, t, d, s \tag{B.4}$$

$$p_{i,r,t,d,s-1} - p_{i,r,t,d,s} \leq \quad Rd_i^{\max} \cdot Hs \cdot Qg_{i,r}^{\text{np}} \cdot (u_{i,r,t,d,s} - su_{i,r,t,d,s}) + \max\left(Pg_i^{\min}, Rd_i^{\max} \cdot Hs\right) \cdot Qg_{i,r}^{\text{np}} \cdot sd_{i,r,t,d,s} \quad \forall\ i \in \mathcal{I}_r^{\text{TH}}, r, t, d, s \tag{B.5}$$

Note that the first terms on the right hand side of (B.4) and (B.5) apply only for normal operating mode (i.e., generator is ON), while the second terms apply for the startup and shutdown modes. This means that generators in normal operating mode have their ramp rates limited by $Ru_i^{\max}$ and $Rd_i^{\max}$, while generators in startup and shutdown modes have their ramp rates limited by the least restrictive between $Pg_i^{\min}$ and $Ru_i^{\max}$, $Rd_i^{\max}$ such that their operating limits (Equations B.6 and B.7) are still satisfied.

The operating limits constraints (B.6)-(B.7) specify that each thermal generator is either OFF and outputting zero power, or ON and running within the operating limits $Pg_i^{\min} \cdot Qg_{i,r}^{\text{np}}$ and $Qg_{i,r}^{\text{np}}$. The variable $u_{i,r,t,d,s}$ (integer variable) represents the number of generators that are ON in cluster $i \in \mathcal{I}_r^{\text{TH}}$ at the time period t, representative day d, and sub-period s.

$$u_{i,r,t,d,s} \cdot Pg_i^{\min} \cdot Qg_{i,r}^{\text{np}} \leq p_{i,r,t,d,s} \qquad \forall\ i \in \mathcal{I}_r^{\text{TH}}, r, t, d, s \tag{B.6}$$

$$p_{i,r,t,d,s} + q_{i,r,t,d,s}^{\text{spin}} \leq u_{i,r,t,d,s} \cdot Qg_{i,r}^{\text{np}} \qquad \forall\ i \in \mathcal{I}_r^{\text{TH}}, r, t, d, s \tag{B.7}$$

The upper limit constraint is modified in order to capture the need for generators to run below the maximum considering operating reserves, where $q_{i,r,t,d,s}^{\text{spin}}$ is a variable representing the spinning reserve capacity.

The total operating reserve constraint (B.8) dictates that the total spinning reserve, $q_{i,r,t,d,s}^{\text{spin}}$, plus quick-start reserve, $q_{i,r,t,d,s}^{\text{Qstart}}$, must exceed the minimum operating reserve, $Op^{\min}$, which is a percentage of the load $L_{r,t,d,s}$ in a reserve

sharing region r at each sub-period s.

$$\sum_{i \in \mathcal{I}_r^{\mathrm{TH}}} \left(q_{i,r,t,d,s}^{\mathrm{spin}} + q_{i,r,t,d,s}^{\mathrm{Qstart}} \right) \geq Op^{\min} \cdot L_{r,t,d,s} \qquad \forall\ r,t,d,s \tag{B.8}$$

Spinning Reserve is the on-line reserve capacity that is synchronized to the grid system and ready to meet electric demand within 10 minutes of a dispatch instruction by the independent system operator (ISO). Quick-start (or non-spinning) reserve is the extra generation capacity that is not currently connected to the system but can be brought on-line after a short delay.

The total spinning reserve constraint (B.9) specifies that the total spinning reserve $q_{i,r,t,d,s}^{\mathrm{spin}}$ must exceed the minimum spinning reserve, $Spin^{\min}$, which is a percentage of the load $L_{r,t,d,s}$ in a reserve sharing region r at each sub-period s.

$$\sum_{i \in \mathcal{I}_r^{\mathrm{TH}}} q_{i,r,t,d,s}^{\mathrm{spin}} \geq Spin^{\min} \cdot L_{r,t,d,s} \qquad \forall\ r,t,d,s \tag{B.9}$$

Our model does not currently impose a minimum requirement for total quick-start reserve, as presented in [11]. However, this constraint could be easily incorporated in the formulation to address the extra secondary (quick-start) reserve requirements needed to account for the increasing short term uncertainty due to more renewable generators contributing to the grid.

The maximum spinning reserve constraint (B.10) states that the maximum fraction of capacity of each generator cluster that can contribute to spinning reserves is given by $Frac_i^{\mathrm{spin}}$, which is a fraction of the nameplate capacity $Qg_{i,r}^{\mathrm{np}}$.

$$q_{i,r,t,d,s}^{\mathrm{spin}} \leq u_{i,r,t,d,s} \cdot Qg_{i,r}^{\mathrm{np}} \cdot Frac_i^{\mathrm{spin}} \qquad \forall\ i \in \mathcal{I}_r^{\mathrm{TH}}, r,t,d,s \tag{B.10}$$

The maximum quick-start reserve constraint dictates that the maximum fraction of the capacity of each generator cluster that can contribute to quick-start reserves is given by $Frac_i^{\mathrm{Qstart}}$ (fraction of the nameplate capacity $Qg_{i,r}^{\mathrm{np}}$), and

that quick-start reserves can only be provided by the generators that are OFF, i.e., not active.

$$q^{\text{Qstart}}_{i,r,t,d,s} \leq (ngo^{\text{th}}_{i,r,t} - u_{i,r,t,d,s}) \cdot Qg^{\text{np}}_{i,r} \cdot Frac^{\text{Qstart}}_{i} \quad \forall\ i \in \mathcal{I}^{\text{TH}}_{r}, r, t, d, s \quad \text{(B.11)}$$

Here the integer variable $ngo^{\text{th}}_{i,r,t}$ represents the number of thermal generators that are operational (i.e., installed and ready to operate) at year t.

B.2 Investment-related constraints

The planning reserve requirement (B.12) ensures that the operating capacity is greater than or equal to the annual peak load $L^{\max}_{t}$, plus a predefined fraction of reserve margin $R^{\min}_{t}$ of the annual peak load $L^{\max}_{t}$.

$$\sum_{i \in \mathcal{I}^{\text{RN}}_{r}} \sum_{r} \left(Qg^{\text{np}}_{i,r} \cdot Q^{\text{v}}_{i} \cdot ngo^{\text{rn}}_{i,r,t}\right) + \sum_{i \in \mathcal{I}^{\text{TH}}_{r}} \sum_{r} \left(Qg^{\text{np}}_{i,r} \cdot ngo^{\text{th}}_{i,r,t}\right) \geq (1 + R^{\min}_{t}) \cdot L^{\max}_{t} \quad \forall\ t \quad \text{(B.12)}$$

For all thermal generators, their full nameplate capacity $Qg^{\text{np}}_{i,r}$ counts towards the planning reserve requirement. However, for the renewable technologies (wind, PV and CSP), their contribution is less than the nameplate due to the inability to control dispatch and the uncertainty of the output [39]. Therefore, the fraction of the capacity that can be reliably counted towards the planning reserve requirement is referred to as the capacity value Q^{v}_{i}.

The minimum annual renewable generation requirement (B.13) ensures that, in case of policy mandates, the renewable generation quota target, $RN^{\min}_{t}$, which is a fraction of the energy demand ED_t, is satisfied. If not, i.e, if there is a deficit def^{rn}_{t} from the quota, this is subjected to a penalty that is included later in the objective function.

$$\sum_{d} \sum_{s} \left[W_d \cdot Hs \cdot \left(\sum_{r} \left(\sum_{i \in \mathcal{I}^{\text{RN}}_{r}} p_{i,r,t,d,s} - cu_{r,t,d,s} \right) \right) \right] + def^{\text{rn}}_{t} \geq RN^{\min}_{t} \cdot ED_t \quad \forall\ t \quad \text{(B.13)}$$

Here W_d represents the weight of the representative day d, Hs is the length of the sub-period, $cu_{r,t,d,s}$ is the curtailment of renewable generation, and ED_t

represent the energy demand in year t:

$$ED_t = \sum_r \sum_d \sum_s (W_d \cdot Hs \cdot L_{r,t,d,s})$$

The maximum yearly installation constraints (B.14)-(B.15) limit the yearly installation per generation type in each region r to an upper bound $Q_{i,t}^{\text{inst,UB}}$ in MW/year. Here $ngb_{i,r,t}^{\text{rn}}$ and $ngb_{i,r,t}^{\text{th}}$ represent the number of renewable and thermal generators built in region r in year t, respectively. Note that due to the flexibility in sizes for renewable generators, $ngb_{i,r,t}^{\text{rn}}$ is relaxed to be continuous.

$$\sum_r ngb_{i,r,t}^{\text{rn}} \leq Q_{i,t}^{\text{inst,UB}} / Qg_{i,r}^{\text{np}} \qquad \forall\ i \in \mathcal{I}_r^{\text{Rnew}}, t \tag{B.14}$$

$$\sum_r ngb_{i,r,t}^{\text{th}} \leq Q_{i,t}^{\text{inst,UB}} / Qg_{i,r}^{\text{np}} \qquad \forall\ i \in \mathcal{I}_r^{\text{Tnew}}, t \tag{B.15}$$

B.3 Generator balance constraints

Concerning renewable generator clusters, we define a set of constraints (B.16)-(B.17) to compute the number of generators in cluster i that are ready to operate $ngo_{i,r,t}^{\text{rn}}$, taking into account the generators that were already existing at the beginning of the planning horizon $Ng_{i,r}^{\text{Rold}}$, the generators built $ngb_{i,r,t}^{\text{rn}}$, and the generators retired $ngr_{i,r,t}^{\text{rn}}$ at year t. It is important to highlight that we assume *no lead time* between the decision to build/install a generator and the moment it can begin producing electricity.

$$ngo_{i,r,t}^{\text{rn}} = Ng_{i,r}^{\text{Rold}} + ngb_{i,r,t}^{\text{rn}} - ngr_{i,r,t}^{\text{rn}} \qquad \forall\ i \in \mathcal{I}_r^{\text{RN}}, r, t = 1 \tag{B.16}$$

$$ngo_{i,r,t}^{\text{rn}} = ngo_{i,r,t-1}^{\text{rn}} + ngb_{i,r,t}^{\text{rn}} - ngr_{i,r,t}^{\text{rn}} \qquad \forall\ i \in \mathcal{I}_r^{\text{RN}}, r, t > 1 \tag{B.17}$$

As aforementioned, due to the flexibility in sizes for renewable generators, $ngo_{i,r,t}^{\text{rn}}$, $ngb_{i,r,t}^{\text{rn}}$, and $ngr_{i,r,t}^{\text{rn}}$ are relaxed to be continuous. Note that $ngb_{i,r,t}^{\text{rn}}$ for $i \in \mathcal{I}_r^{\text{Rold}}$ is fixed to zero in all time periods, i.e., the clusters of existing renewable generators cannot have any new additions during the time horizon considered.

We also define a set of constraints (B.18) to enforce the renewable generators

that reached the end of their lifetime to either retire, $ngr^{\mathrm{rn}}_{i,r,t}$, or have their life extended, $nge^{\mathrm{rn}}_{i,r,t}$. $Ng^{\mathrm{r}}_{i,r,t}$ is a parameter that represents the number of old generators (i.e., $i \in \mathcal{I}^{\mathrm{old}}_r$) that reached the end of their lifetime, LT_i, at year t. We assume that the new renewable generators will not need to retire within the planning horizon.

$$Ng^{\mathrm{r}}_{i,r,t} = ngr^{\mathrm{rn}}_{i,r,t} + nge^{\mathrm{rn}}_{i,r,t} \qquad \forall\ i \in \mathcal{I}^{\mathrm{Rold}}_r, r, t \tag{B.18}$$

Concerning thermal generator clusters, we define a set of constraints (B.19)-(B.20) to compute the number of generators in cluster i that are ready to operate $ngo^{\mathrm{th}}_{i,r,t}$, taking into account the generators that were already existing at the beginning of the planning horizon $Ng^{\mathrm{Told}}_{i,r}$, the generators built $ngb^{\mathrm{th}}_{i,r,t}$, and the generators retired $ngr^{\mathrm{th}}_{i,r,t}$ at year t.

$$ngo^{\mathrm{th}}_{i,r,t} = Ng^{\mathrm{Told}}_{i,r} + ngb^{\mathrm{th}}_{i,r,t} - ngr^{\mathrm{th}}_{i,r,t} \qquad \forall\ i \in \mathcal{I}^{\mathrm{TH}}_r, r, t = 1 \tag{B.19}$$

$$ngo^{\mathrm{th}}_{i,r,t} = ngo^{\mathrm{th}}_{i,r,t-1} + ngb^{\mathrm{th}}_{i,r,t} - ngr^{\mathrm{th}}_{i,r,t} \qquad \forall\ i \in \mathcal{I}^{\mathrm{TH}}_r, r, t > 1 \tag{B.20}$$

Note that $ngb^{\mathrm{th}}_{i,r,t}$ for $i \in \mathcal{I}^{\mathrm{Told}}_r$ is fixed to zero in all time periods, i.e., the clusters of existing thermal generators cannot have any new additions during the time horizon considered.

We also define a set of constraints (B.21) to enforce the thermal generators that reached the end of their lifetime to either retire, $ngr^{\mathrm{th}}_{i,r,t}$, or have their life extended $nge^{\mathrm{th}}_{i,r,t}$. We assume that the new thermal generators will not need to retire within the planning horizon.

$$Ng^{\mathrm{r}}_{i,r,t} = ngr^{\mathrm{th}}_{i,r,t} + nge^{\mathrm{th}}_{i,r,t} \qquad \forall\ i \in \mathcal{I}^{\mathrm{Told}}_r, r, t \tag{B.21}$$

Finally, we have constraint (B.22) that ensures that only installed generators can be in operation:

$$u_{i,r,t,d,s} \leq ngo^{\mathrm{th}}_{i,r,t} \qquad \forall\ i \in \mathcal{I}^{\mathrm{Tnew}}_r, r, t, d, s \tag{B.22}$$

B.4 Storage constraints

We also include a set constraints related to the energy storage devices, which are assumed to be ideal and generic [45]. Constraints (B.23)-(B.24) compute the number of storage units that are ready to operate $nso_{j,r,t}$, taking into account the storage units already existing at the beginning of the planning horizon $Ns_{j,r}$ and the ones built $nsb_{j,r,t}$ and retired $nsr_{j,r,t}$ at year t. Due to the flexibility in sizes for storage units, $nso_{j,r,t}$, $nsb_{j,r,t}$, and $nsr_{j,r,t}$ are relaxed to be continuous.

$$nso_{j,r,t} = Ns_{j,r} + nsb_{j,r,t} - nsr_{s,r,t} \qquad \forall\ j,r,t=1 \tag{B.23}$$

$$nso_{j,r,t} = nso_{j,r,t-1} + nsb_{j,r,t} - nsr_{j,r,t} \qquad \forall\ j,r,t>1 \tag{B.24}$$

Constraints (B.25) and (B.26) establish that the power charge, $p^{\text{charge}}_{j,r,t,d,s}$, and discharge, $p^{\text{discharge}}_{j,r,t,d,s}$, of the storage units in cluster j, $nso_{j,r,t}$, has to be within the operating limits: $Charge^{\min}_{j}$ and $Charge^{\max}_{j}$, and $Discharge^{\min}_{j}$ and $Discharge^{\min}_{j}$, respectively.

$$Charge^{\min}_{j} \cdot nso_{j,r,t} \leq p^{\text{charge}}_{j,r,t,d,s} \leq Charge^{\max}_{j} \cdot nso_{j,r,t} \qquad \forall\ j,r,t,d,s \tag{B.25}$$

$$Discharge^{\min}_{j} \cdot nso_{j,r,t} \leq p^{\text{discharge}}_{j,r,t,d,s} \leq Discharge^{\max}_{j} \cdot nso_{j,r,t} \quad \forall\ j,r,t,d,s \tag{B.26}$$

Constraint (B.27) specifies that the energy storage level, $p^{\text{level}}_{j,r,t,d,s}$, for the storage units in cluster j, $nso_{j,r,t}$ has to be within the storage capacity limits $Storage^{\min}_{j}$ and $Storage^{\max}_{j}$.

$$Storage^{\min}_{j} \cdot nso_{j,r,t} \leq p^{\text{level}}_{j,r,t,d,s} \leq Storage^{\max}_{j} \cdot nso_{j,r,t} \quad \forall\ j,r,t,d,s \tag{B.27}$$

Constraints (B.28) and (B.29) show the power balance in the storage units. The state of charge $p^{\text{level}}_{j,r,t,d,s}$ at the end of sub-period s depends on the previous state of charge $p^{\text{level}}_{j,r,t,d,s-1}$, and the power charged $p^{\text{charge}}_{j,r,t,d,s}$ and discharged $p^{\text{discharge}}_{j,r,t,d,s}$ at sub-period s. The symbols η^{charge}_{j} and $\eta^{\text{discharge}}_{j}$ represent the charg-

ing and discharging efficiencies, respectively. For the first hour of the day d of year t, the previous state of charge (i.e., $s = 0$) is the variable $p^{\text{level,0}}_{j,r,t,d}$.

$$p^{\text{level}}_{j,r,t,d,s} = p^{\text{level}}_{j,r,t,d,s-1} + \eta^{\text{charge}}_{j} \cdot p^{\text{charge}}_{j,r,t,d,s} + p^{\text{discharge}}_{j,r,t,d,s} / \eta^{\text{discharge}}_{j} \quad \forall\ j, r, t, d, s > 1 \tag{B.28}$$

$$p^{\text{level}}_{j,r,t,d,s} = p^{\text{level,0}}_{j,r,t,d} + \eta^{\text{charge}}_{j} \cdot p^{\text{charge}}_{j,r,t,d,s} + p^{\text{discharge}}_{j,r,t,d,s} / \eta^{\text{discharge}}_{j} \quad \forall\ j, r, t, d, s = 1 \tag{B.29}$$

Constraints (B.30) and (B.31) force the storage units to begin $p^{\text{level,0}}_{j,r,t,d}$ and end $p^{\text{level}}_{j,r,t,d,s=S}$ each day d of year t with 50% of their maximum storage $Storage^{\max}_{j}$. This is a heuristic to attach carryover storage level form one representative day to the next.

$$p^{\text{level,0}}_{j,r,t,d} = 0.5 \cdot Storage^{\max}_{j} \cdot nso_{j,r,t} \quad \forall\ j, r, t, d \tag{B.30}$$

$$p^{\text{level}}_{j,r,t,d,s} = 0.5 \cdot Storage^{\max}_{j} \cdot nso_{j,r,t} \quad \forall\ j, r, t, d, s = S \tag{B.31}$$

B.5 Objective Function

The objective of this model is to minimize the net present cost, Φ, over the planning horizon, which includes operating costs Φ^{opex}, investment costs Φ^{capex}, and potential penalties Φ^{PEN} for not meeting the the targets on renewables.

$$\min \quad \Phi = \sum_{t} \left(\Phi^{\text{opex}}_{t} + \Phi^{\text{capex}}_{t} + \Phi^{\text{PEN}}_{t} \right) \tag{B.32}$$

The operating expenditure, Φ^{opex}_{t}, comprises the variable $VOC_{i,t}$ and fixed $FOC_{i,t}$ operating costs, as well as fuel cost P^{fuel}_{i} per heat rate HR_i, carbon tax $Tx^{\text{CO}_2}_{t}$ for CO_2 emissions $EF^{CO_2}_{i}$, and start-up cost (variable cost P^{fuel}_{i} that depends on the amount of fuel burned for startup F^{start}_{i}, and fixed cost C^{start}_{i}).

$$
\begin{aligned}
\Phi_t^{\text{opex}} = \quad & If_t \cdot \Bigg[\sum_d \sum_s W_d \cdot hs \cdot \\
& \left(\sum_i \sum_r (VOC_{i,t} + P_i^{\text{fuel}} \cdot HR_i + Tx_t^{\text{CO}_2} \cdot EF_i^{CO_2} \cdot HR_i) \cdot p_{i,r,t,d,s} \right) \\
& + \left(\sum_{i \in \mathcal{I}_r^{\text{RN}}} \sum_r FOC_{i,t} \cdot Qg_{i,r}^{\text{np}} \cdot ngo_{i,r,t}^{\text{rn}} \right) \\
& + \left(\sum_{i \in \mathcal{I}_r^{\text{TH}}} \sum_r FOC_{i,t} \cdot Qg_{i,r}^{\text{np}} \cdot ngo_{i,r,t}^{\text{th}} \right) \\
& + \sum_{i \in \mathcal{I}_r^{\text{TH}}} \sum_r \sum_d \sum_s W_d \cdot Hs \cdot su_{i,r,t,d,s} \cdot Qg_{i,r}^{\text{np}} \\
& \cdot \left(F_i^{\text{start}} \cdot P_i^{\text{fuel}} + F_i^{\text{start}} \cdot EF^{CO_2} \cdot Tx_t^{\text{CO}_2} + C_i^{\text{start}} \right) \Bigg]
\end{aligned}
\tag{B.33}
$$

The capital expenditure, Φ_t^{capex}, includes the amortized cost of acquiring new generators, $DIC_{i,t}$, new storage devices, $SIC_{j,t}$, and the amortized cost of extending the life of generators that reached their expected lifetime, the amortized cost of building new transmission lines $TIC_{l,t}$. The cost of extending the life of a generator is assumed to be a fraction LE_i of the investment cost, $DIC_{i,t}$, in a new generator with the same or equivalent generation technology. In this framework, the investment cost takes into account the remaining value at the end of the time horizon by considering the annualized capital cost and multiplying it by the number of years remaining in the planning horizon at the time

of installation to calculate the $DIC_{i,t}$.

$$\begin{aligned}\Phi_t^{\text{capex}} = \quad If_t \cdot \Bigg[& \sum_{i \in \mathcal{I}_r^{\text{Rnew}}} \sum_r DIC_{i,t} \cdot CC_i^{\text{m}} \cdot Qg_{i,r}^{\text{np}} \cdot ngb_{i,r,t}^{\text{rn}} \\ & + \sum_{i \in \mathcal{I}_r^{\text{Tnew}}} \sum_r DIC_{i,t} \cdot CC_i^{\text{m}} \cdot Qg_{i,r}^{\text{np}} \cdot ngb_{i,r,t}^{\text{th}} \\ & + \sum_j \sum_r SIC_{j,t} \cdot Storage_j^{\max} \cdot nsb_{j,r,t} \\ & + \sum_{i \in \mathcal{I}_r^{\text{RN}}} \sum_r DIC_{i,t} \cdot LE_i \cdot Qg_{i,r}^{\text{np}} \cdot nge_{i,r,t}^{\text{rn}} \\ & + \sum_{i \in \mathcal{I}_r^{\text{TH}}} \sum_r DIC_{i,t} \cdot LE_i \cdot Qg_{i,r}^{\text{np}} \cdot nge_{i,r,t}^{\text{th}} \\ & + \sum_{l \in \mathcal{L}^{\text{new}}} \sum_t TIC_{l,t} \cdot ntb_{l,t} \Bigg]\end{aligned} \tag{B.34}$$

The capital multiplier CC_i^{m} associated with new generator clusters is meant to account for differences in depreciation schedules applicable to each technology, with higher values being indicative of slower depreciating schedule and vice versa.

Lastly, the penalty cost, Φ_t^{PEN}, includes the potential fines for not meeting the renewable energy quota, PEN_t^{rn}, and curtailing the renewable generation.

$$\Phi_t^{\text{PEN}} = \quad If_t \cdot \left(PEN_t^{\text{rn}} \cdot def_t^{\text{rn}} + PEN^{\text{c}} \cdot \sum_r \sum_d \sum_s cu_{r,t,d,s} \right) \tag{B.35}$$

Calculated parameters

The parameters If_t, $DIC_{i,t}$, $ACC_{i,t}$, and T_t^{remain} are defined as follows. Regarding the parameters used in equations (B.33)-(B.35), the discount factor in year t, If_t, is calculated from the interest rate, Ir:

$$If_t = \frac{1}{(1+Ir)^t}$$

and the discounted investment cost $DIC_{i,t}$ is given by:

$$DIC_{i,t} = ACC_{i,t} \cdot \left(\sum_{t' \leq \min(LT_i, T^{\text{remain}})} If_{t'} \right)$$

where the annualized capital cost $ACC_{i,t}$ is given by:

$$ACC_{i,t} = \frac{OCC_{i,t} \cdot Ir}{1 - \frac{1}{(1+Ir)^{LT_i}}}$$

and the remaining time in the horizon T_t^{remain} is defined by $T_t^{\text{remain}} = T - t + 1$. The discounted investment cost of the transmission lines $TIC_{l,t}$ can be calculated similarly.

Acknowledgements

The authors gratefully acknowledge financial support from the Center of Advanced Process Decion-making at Carnegie Mellon University and from the Department of Energy as part of the IDAES Project. Can Li would like to thank Dr. Cristiana Lara for providing some of the input data and the Python/Pyomo code for the GEP model.

[1] A. J. Conejo, L. Baringo, S. J. Kazempour, A. S. Sissiqui, Investment in Electricity Generation and Transmission - Decision Making under Uncertainty, Springer International Publishing, 2016. doi:10.1007/978-3-319-29501-5.

[2] N. E. Koltsaklis, A. S. Dagoumas, State-of-the-art generation expansion planning: A review, Applied Energy 230 (2018) 563–589.

[3] C. L. Lara, D. S. Mallapragada, D. J. Papageorgiou, A. Venkatesh, I. E. Grossmann, Deterministic electric power infrastructure planning: Mixed-integer programming model and nested decomposition algorithm, European Journal of Operational Research 271 (3) (2018) 1037–1054.

[4] H. Sadeghi, M. Rashidinejad, A. Abdollahi, A comprehensive sequential review study through the generation expansion planning, Renewable and Sustainable Energy Reviews 67 (2017) 1369–1394.

[5] V. Oree, S. Z. S. Hassen, P. J. Fleming, Generation expansion planning optimisation with renewable energy integration: A review, Renewable and Sustainable Energy Reviews 69 (2017) 790–803.

[6] J. Ding, A. Somani, A long-term investment planning model for mixed energy infrastructure integrated with renewable energy, in: 2010 IEEE Green Technologies Conference, 2010, pp. 1–10. doi:10.1109/GREEN.2010.5453785.

[7] N. E. Koltsaklis, M. C. Georgiadis, A multi-period, multi-regional generation expansion planning model incorporating unit commitment constraints, Applied Energy 158 (2015) 310 – 331. doi:http://dx.doi.org/10.1016/j.apenergy.2015.08.054.
URL http://www.sciencedirect.com/science/article/pii/S0306261915009873

[8] A. Pina, C. A. Silva, P. Ferrão, High-resolution modeling framework for planning electricity systems with high penetration of renewables, Applied Energy 112 (2013) 215 – 223. doi:http://dx.doi.org/10.1016/j.apenergy.2013.05.074.
URL http://www.sciencedirect.com/science/article/pii/S030626191300487X

[9] K. Poncelet, E. Delarue, J. Duerinck, D. Six, W. D'haeseleer, The importance of integrating the variability of renewables in long-term energy planning models, KU Leuven (2014) 1–18.
URL https://www.mech.kuleuven.be/en/tme/research/energy_environment/Pdf/wp-importance.pdf

[10] A. Shortt, M. O'Malley, Impact of variable generation in generation re-

source planning models, in: IEEE PES General Meeting, 2010, pp. 1–6. doi:10.1109/PES.2010.5589461.

[11] A. Flores-Quiroz, R. Palma-Behnke, G. Zakeri, R. Moreno, A column generation approach for solving generation expansion planning problems with high renewable energy penetration, Electric Power Systems Research 136 (2016) 232 – 241. doi:http://dx.doi.org/10.1016/j.epsr.2016.02.011.
URL http://www.sciencedirect.com/science/article/pii/S0378779616300177

[12] B. Palmintier, M. Webster, Impact of unit commitment constraints on generation expansion planning with renewables, in: 2011 IEEE power and energy society general meeting, IEEE, 2011, pp. 1–7.

[13] T. Lohmann, S. Rebennack, Tailored Benders decomposition for a long-term power expansion model with short-term demand response, Management Science 63 (6) (2017) 2027–2048.

[14] L. Bahiense, G. C. Oliveira, M. Pereira, S. Granville, A mixed integer disjunctive model for transmission network expansion, IEEE Transactions on Power Systems 16 (3) (2001) 560–565.

[15] N. Alguacil, A. L. Motto, A. J. Conejo, Transmission expansion planning: a mixed-integer LP approach, IEEE Transactions on Power Systems 18 (3) (2003) 1070–1077. doi:10.1109/TPWRS.2003.814891.

[16] H. Zhang, G. T. Heydt, V. Vittal, J. Quintero, An improved network model for transmission expansion planning considering reactive power and network losses, IEEE Transactions on Power Systems 28 (3) (2013) 3471–3479.

[17] R. Hemmati, R.-A. Hooshmand, A. Khodabakhshian, State-of-the-art of transmission expansion planning: Comprehensive review, Renewable and Sustainable Energy Reviews 23 (2013) 312–319.

[18] V. Krishnan, J. Ho, B. F. Hobbs, A. L. Liu, J. D. McCalley, M. Shahidehpour, Q. P. Zheng, Co-optimization of electricity transmission and generation resources for planning and policy analysis: review of concepts and modeling approaches, Energy Systems 7 (2) (2016) 297–332. doi:10.1007/s12667-015-0158-4.

[19] D. Pozo, E. E. Sauma, J. Contreras, A three-level static MILP model for generation and transmission expansion planning, IEEE Transactions on Power systems 28 (1) (2012) 202–210.

[20] J. Aghaei, N. Amjady, A. Baharvandi, M.-A. Akbari, Generation and transmission expansion planning: MILP–based probabilistic model, IEEE Transactions on Power Systems 29 (4) (2014) 1592–1601.

[21] C. L. Lara, J. D. Siirola, I. E. Grossmann, Electric power infrastructure planning under uncertainty: stochastic dual dynamic integer programming (sddip) and parallelization scheme, Optimization and Engineering (2019) 1–39.

[22] R. P. O'Neill, E. A. Krall, K. W. Hedman, S. S. Oren, A model and approach to the challenge posed by optimal power systems planning, Mathematical Programming 140 (2) (2013) 239–266. doi:10.1007/s10107-013-0695-3.
URL http://dx.doi.org/10.1007/s10107-013-0695-3

[23] Y. Liu, R. Sioshansi, A. J. Conejo, Multistage stochastic investment planning with multiscale representation of uncertainties and decisions, IEEE Transactions on Power Systems 33 (1) (2017) 781–791.

[24] D. Mejía-Giraldo, J. D. McCalley, Maximizing future flexibility in electric generation portfolios, IEEE Transactions on Power Systems 29 (1) (2013) 279–288.

[25] L. Baringo, A. Baringo, A stochastic adaptive robust optimization approach

for the generation and transmission expansion planning, IEEE Transactions on Power Systems 33 (1) (2017) 792–802.

[26] H. Le Cadre, A. Papavasiliou, Y. Smeers, Wind farm portfolio optimization under network capacity constraints, European Journal of Operational Research 247 (2) (2015) 560–574.

[27] D. S. Mallapragada, D. J. Papageorgiou, A. Venkatesh, C. L. Lara, I. E. Grossmann, Impact of model resolution on scenario outcomes for electricity sector system expansion, Energy 163 (2018) 1231–1244.

[28] H. Teichgraeber, A. R. Brandt, Clustering methods to find representative periods for the optimization of energy systems: An initial framework and comparison, Applied Energy 239 (2019) 1283–1293.

[29] I. J. Scott, P. M. Carvalho, A. Botterud, C. A. Silva, Clustering representative days for power systems generation expansion planning: Capturing the effects of variable renewables and energy storage, Applied Energy 253 (2019) 113603.

[30] I. E. Grossmann, F. Trespalacios, Systematic modeling of discrete-continuous optimization models through generalized disjunctive programming, AIChE Journal 59 (9) (2013) 3276–3295.

[31] J. R. Birge, Decomposition and partitioning methods for multistage stochastic linear programs, Operations Research 33 (5) (1985) 989–1007. arXiv:http://dx.doi.org/10.1287/opre.33.5.989, doi:10.1287/opre.33.5.989.
URL http://dx.doi.org/10.1287/opre.33.5.989

[32] J. Zou, S. Ahmed, X. A. Sun, Stochastic dual dynamic integer programming, Mathematical Programming 175 (1-2) (2019) 461–502.

[33] R. Rahmaniani, T. G. Crainic, M. Gendreau, W. Rei, The Benders decomposition algorithm: A literature review, European Journal of Operational Research 259 (3) (2016) 801–817.

doi:http://dx.doi.org/10.1016/j.ejor.2016.12.005.
URL http://www.sciencedirect.com/science/article/pii/S0377221716310244

[34] P. Bonami, D. Salvagnin, A. Tramontani, Implementing automatic Benders decomposition in a modern MIP solver.
URL http://www.dei.unipd.it/~salvagni/pdf/CPXbenders.pdf

[35] A. B. Birchfield, T. Xu, K. M. Gegner, K. S. Shetye, T. J. Overbye, Grid structural characteristics as validation criteria for synthetic networks, IEEE Transactions on power systems 32 (4) (2016) 3258–3265.

[36] J. Andrade, R. Baldick, Estimation of transmission costs for new generation, White Paper UTEI/2016-08-1.
URL http://sites.utexas.edu/energyinstitute/files/2016/11/UTAustin_FCe_TransmissionCosts_2016.pdf

[37] W. Cole, P. Kurup, M. Hand, D. Feldman, B. Sigrin, E. Lantz, T. Stehly, C. Augustine, C. Turchi, P. O'Connor, et al., 2016 annual technology baseline (atb), Tech. rep., National Renewable Energy Lab.(NREL), Golden, CO (United States) (2016).

[38] U.S. Energy Information Administration, Annual Energy Outlook 2019, https://www.eia.gov/outlooks/aeo/pdf/aeo2019.pdf (2019).

[39] W. Short, P. Sullivan, T. Mai, M. Mowers, C. Uriarte, N. Blair, D. Heimiller, A. Martinez, Regional energy deployment system (reeds), Tech. Rep. December, National Renewable Technology Laboratory (NREL) (2011). doi:NREL/TP-6A20-46534.
URL https://www.nrel.gov/analysis/reeds/pdfs/reeds_documentation.pdf

[40] M. Sengupta, Y. Xie, A. Lopez, A. Habte, G. Maclaurin, J. Shelby, The national solar radiation data base (nsrdb), Renewable and Sustainable Energy Reviews 89 (2018) 51–60.

[41] N. Blair, A. P. Dobos, J. Freeman, T. Neises, M. Wagner, T. Ferguson, P. Gilman, S. Janzou, System advisor model, sam 2014.1. 14: General description, Tech. rep., National Renewable Energy Lab.(NREL), Golden, CO (United States) (2014).

[42] C. Draxl, A. Clifton, B.-M. Hodge, J. McCaa, The wind integration national dataset (wind) toolkit, Applied Energy 151 (2015) 355–366.

[43] W. E. Hart, J.-P. Watson, D. L. Woodruff, Pyomo: modeling and solving mathematical programs in python, Mathematical Programming Computation 3 (3) (2011) 219.

[44] J. D. Siirola, Pyomo: Introdection & idaes development., Tech. rep., Sandia National Lab.(SNL-NM), Albuquerque, NM (United States) (2017).

[45] D. Pozo, J. Contreras, E. E. Sauma, Unit commitment with ideal and generic energy storage units, IEEE Transactions on Power Systems 29 (6) (2014) 2974–2984. doi:10.1109/TPWRS.2014.2313513.